Regulation of SLIT-Robo Signaling by Scaffolding Proteins

Bret K. Samelson

A dissertation

submitted in partial fulfillment of the

requirement for the degree of

Doctor of Philosophy

University of Washington

2015

Reading Committee:

John Scott, Chair

Stanley McKnight

Luis Fernando Santana

Program authorized to offer degree:

Pharmacology

University of Washington

Abstract

Regulation of SLIT-Robo Signaling by Scaffolding Proteins

Bret K. Samelson

Chair of the Supervisory Committee:
Professor John D. Scott
Department of Pharmacology

Axon guidance receptors in the growth cone respond to secreted molecular cues, directing axons towards their appropriate targets of innervation. Many of these receptors complex with scaffolding proteins which recruit protein kinases and protein phosphatases to control the efficacy, context, and duration of neuronal phosphorylation events. The A-Kinase Anchoring Protein AKAP79/150 interacts with protein kinase A (PKA), protein kinase C (PKC), and protein phosphatase 2B (PP2B, calcineurin) to modulate second messenger signaling events. In a mass spectrometry based screen for additional AKAP79/150 binding partners, we have identified the Roundabout axonal guidance receptor Robo2 and its ligands Slit2 and Slit3. Biochemical and cellular approaches confirm that a linear sequence located in the cytoplasmic tail of Robo2 (residues 991-1070) interfaces directly with sites on the anchoring protein. Additional studies show that AKAP79/150 interacts with the Robo3 receptor in a similar manner. Immunofluorescent staining detects overlapping expression patterns for murine AKAP150, Robo2, and Robo3 in a variety of brain regions including hippocampal region CA1 and the islands of calleja. In vitro kinase assays, peptide spot array

mapping, and proximity ligation assay staining approaches establish that human AKAP79-anchored PKC selectively phosphorylates the Robo3.1 receptor subtype on serine 1330. In a parallel set of experiments, we also identified an interaction between Robo3 and the 14-3-3 family of adaptor proteins. Binding between these proteins can be disrupted using the R18 14-3-3 competitor peptide, confirming the specificity of this interaction. In addition, PKC activation decreases the binding of 14-3-3 to the Robo3 receptor. These finding suggest that scaffolding proteins interact with specific Robo receptor subcomplexes, providing enhanced regulation of this family of axon guidance molecules.

Table of Contents

List of Figures:

List of Abbreviations:

Abbreviation	Full name
Abl	Abelson tyrosine kinase
AC	Adenylyl cyclase
AKAP	A-kinase anchoring protein
ALPS	Agrin-Laminin-Perlecan-Slit
AMPA	α-amino-3-hydroxy-5-methylisooxazole-4-propionic acid
BIS I	Bisindolylmaleimide I
cAMP	Cyclic adenosine monophosphate
CAP	Cyclase-associated protein
Cdc42	Cell division control protein 42 homolog
CrGAP	Cross GTPase activating protein
CXCR4	C-X-C chemokine receptor type 4
DCC	Deleted in colorectal cancer
EGF	Epidermal growth factor
Ena	Enabled protein
FN	Fibronectin
GABA	Gamma-aminobutyric acid
Ig	Immunoglobulin
JNK	Jun N-terminal protein kinase
KO	Knockout
LRR	Leucine-rich region
LTD	Long-term depression
LTP	Long-term potentiation
M1	M_1 muscarinic receptor
NMDA	N-methyl D-aspartate
PAK	p21-activated kinase
PDBu	Phorbol 12, 13-dibutyrate
PKA	Protein kinase A
PKC	Protein kinase C
PP1	Protein phosphatase 1
Rac1	Ras-related C3 botulinum toxin substrate 1
RhoA	Ras homolog gene family, member A
RII	PKA regulatory subunit type II
Robo	Roundabout
SDF-1	Stromal cell-derived factor 1
SOS	Son of sevenless
SRGAP	Slit-Robo Rho GTPase-activating protein
VASP	Vasodilator-stimulated phosphoprotein

Acknowledgements

First, I would like to thank John Scott for all of his support throughout my graduate career and for giving me the freedom to work on interesting questions. Thanks as well to my thesis committee members Jim Bruce, Rich Gardner, Stan McKnight, and Fernando Santana for all of your helpful advice. I would also like to acknowledge all present and former members of the Scott lab. It's been a pleasure to work with such great people and I'm so grateful to have had the opportunity to learn from each of you. Specifically, I'd like to thank Donelson Smith and Dave Canton for their guidance on the work described in this thesis. My graduate school experience also wouldn't have been nearly as much fun without my fellow graduate students Patrick Nygren and Jen Whiting, who always kept my mood up. Finally, thanks to my parents, friends, and Sachi Seilie for your love and support.

Preface

Portions of the text and data from this dissertation are reproduced from the following previously published work under fair use:

Samelson BK, Gore BB, Whiting JL, Nygren PJ, Purkey AM, Colledge M, Langeberg LK, Dell'Acqua ML, Zweifel LS, Scott JD. A-Kinase Anchoring Protein 79/150 recruits Protein Kinase C to phosphorylate Roundabout receptors. *J. Biol. Chem (in press)*

Chapter 1: Introduction to Slit-Robo Signaling

As the nervous system develops, large numbers of neurons send out projections that must migrate to precise locations and synapse onto other cells. Secreted guidance cues either attract or repel axons by binding to receptors in axonal and dendritic growth cones (1). Attractive cues promote actin polymerization and stimulate growth cones to move towards a given target. Cues signaling repulsion collapse the growth cone and cause axons to turn away from the gradient of secreted protein.

Roundabout receptors were among the first proteins discovered to play a role in axonal repulsion. Robos were initially identified in a forward genetic screen looking for genes regulating midline crossing in drosophila (2). During midline crossing, axons are drawn to the midline by chemoattractants such as Netrin that are secreted by the floor plate (3). However, after entering the midline migrating axons must be directed away from this potent source of attractive cues and subsequently prevented from recrossing. Loss of Robo function leads to a number of defects in midline crossing (4). First, many ipsilateral axons that would normally project along the midline now cross this structure. In addition, a large number of axons exhibited repeated crossing and recrossing behavior. It was subsequently determined that the Slit family of proteins are the ligands for Robo receptors (5,6). Three mammalian Slit proteins have been identified. While the Slit homologs differ in expression patterns and proteolytic processing, all share

the ability to bind Robos. Slit binding to Robo receptors triggers actin depolymerization in the growth cone and repels migrating axons (7).

The Robo family consists of four members: Robo1, Robo2, Robo3, and Robo4 (8). The functions of Robo1-3 have been extensively characterized in the nervous system. In contrast, Robo4 expression appears to be restricted to the vascular endothelium where it inhibits cell migration (9). Robo1 and Robo2 function in a similar manner and are conventional Robo receptors involved in repulsive signaling. While mice lacking these receptors do not survive to adulthood, much has been learned by examining the embryonic phenotypes of Robo1 and Robo2 KO animals. Robo1 KO mice exhibit guidance defects such as the dorsal projection of axons out of the floor plate (10). In addition, both Robo1 -/- and Robo2 -/- animals show alterations in the development of the lateral and ventral funiculi. As Robo1 and Robo2 can partially compensate for loss of the other receptor, more dramatic phenotypes are evident in Robo1/2 double knockout mice (11). This work has revealed that loss of both of these receptors causes a substantial number of axons to aberrantly project into the contralateral grey matter of the developing spinal cord.

Characterization of Robo1 and Robo2 receptors raised the question of how Slit-Robo signaling is suppressed prior to midline crossing. Without some system to block premature repulsion, axons would not be able to properly respond to the chemoattractants drawing them to the midline. Early proposals included

downregulation of Robo1/2 expression prior to crossing as well as the presence of additional signaling pathways that could inhibit repulsive Robo signaling (12). Both of these explanations appear to be correct. In vertebrates, Robo3 functions to suppress Robo1/2 signaling prior to crossing (13). Vertebrate Robo3 functions in a completely distinct manner from the other Robo receptors. Firstly, Robo3 does not have the ability to bind Slit ligands (14). In mice and other vertebrates, Robo3 serves to inhibit repulsive signaling through Robo1 and Robo2 through an unknown mechanism.

In addition to their role in controlling midline crossing for commissural axons, Robos also function in longitudinal pathway selection. Postcrossing axons migrate along a series of tracts parallel to the ventral midline. Work in Drosophila has revealed that the combination of Robo receptors expressed in an axonal growth cone determines whether that axon will travel to the medial, intermediate, or lateral longitudinal fascicle (15). Expression of Robo1 alone directs axons medial to the midline, whereas Robo2 and Robo3 promote increasingly lateral positioning. Thus, Robos are involved in guiding axons to their ultimate destinations even after the process of midline crossing is complete.

Allele swapping experiments in Drosophila suggest that the apparent differences in function between Robo family members are due to a number of factors. These include distinct expression patterns, differing ectodomains, as well as divergent intracellular C-termini (16-18). Differences in expression patterns and

ectodomain structure are largely responsible for each Robo family member's ability to direct axons to distinct longitudinal pathways. However, there is strong evidence that the unique ability of Robo3 to silence Slit-Robo repulsion is dependent on its C-terminus (19). Furthermore, C-terminal differences likewise contribute to subtle differences between Robo1 and Robo2 in regulating midline crossing.

Slit and Robo proteins are also expressed in other regions of the developing nervous system. For instance, they play an essential role in guiding retinal ganglion cell axons as they negotiate crossing of the optic chiasm (20). Other areas shown to contain axons responsive to Slit include the olfactory bulb, cortex, and hippocampus (7). In many of these brain regions, Robo expression is not restricted to axons and these receptors have been found to play an important role in the regulation of dendritic development. Slit treatment of cortical neurons results in the stimulation of dendritic branching (21). Studies using dominant negative mutants of Robo1 and Robo2 confirm that both receptors are involved in this Slit-induced effect. Recent work has also suggested that Slit-Robo signaling is required for dendritic self-avoidance (22). In cerebellar Purkinje cells, this is due to signaling through Robo2. Thus, Robos seem to play a role in multiple aspects of synaptic development.

Intriguingly, Robo receptors continue to be expressed in many brain regions after development is complete (23). While it has been proposed that these proteins

may regulate synaptic plasticity, this hypothesis has not been extensively tested. Outside of the nervous system, Robo receptors have been shown to direct bud formation in the kidney and misregulation of Slit-Robo signaling has also been implicated in cancerous transformation (24,25).

Efforts to characterize Slit-Robo signaling in the nervous systems have utilized a number of model organisms including drosophila, zebrafish, and mice. While studies in each species have yielded critical results, it is important to note that differences in Robo signaling exist between species. These are particularly striking for the function of the Robo3 receptor. In drosophila, Robo3 does not silence Slit repulsion, but instead functions similarly to Robo1 and Robo2 (12). Another protein, Commissureless, inhibits Robo1 and Robo2 prior to midline crossing (26). Commissureless is not present in vertebrates. These results highlight the need to interpret data on receptor function within the context of Slit-Robo signaling for each model organism.

Roundabout receptors are single pass transmembrane proteins belonging to the immunoglobulin superfamily and consist of an ectodomain and intracellular C-terminus (27). The ectodomain of vertebrate Robos consists of three fibronectin (FN) three repeats and five immunoglobulin (Ig) domains. Slit binding is mediated by interactions between the first two Ig domains of Robo and the second leucine rich-repeat (LRR) domain of Slit (28). Heparan sulfate proteoglycans also function in stabilizing this interaction (29). The intracellular tails of Robo receptors

consist of a series of up to four conserved regions (CC0-3) and are considerably more divergent than the ectodomains. For example, vertebrate Robo3 lacks the CC1 region (30).

Slits are large secreted glycoproteins present in the extracellular matrix. They can be proteolytically processed into an N-terminal 140 kDa fragment and a 60 kDa C-terminal cleavage product (31). Only the N-terminal fragment appears to retain the ability to repulse axonal growth cones. Slits are composed of four amino-terminal LRR domains involved in Robo binding, as well as a variable number of EGF repeats, and an Agrin-Laminin-Perlecan-Slit (ALPS) spacer (32). Slit proteins in solution exist predominantly in a dimeric form and the dimerization interface has been mapped to the fourth LRR domain. While dimerization is not essential for Slit repulsion, it appears to enhance this effect (33).

Mouse studies utilizing Slit -/- animals have demonstrated that the three Slit proteins have functional redundancies. Individual Slit1, Slit2, or Slit3 null animals exhibit minor axonal guidance defects in specific regions of the brain and spinal cord. However, it is only in Slit double or triple KO mice that axons fail to leave the midline or exhibit recrossing defects (10).

Slit1/2/3 -/- animals phenocopy many of the defects found in Robo1/2-deficient mice. However, there are some differences. For example, the degree of axonal stalling observed when commissural axons attempt to cross the midiline is less

severe in Robo1/2 knockouts compared to Slit TKO animals (11). In addition, defasciculation of precrossing axons is observed for Slit TKO, but not Robo1/2 null mice. These discrepancies suggest the presence of one or more additional neuronal receptors capable of binding Slit proteins. Recent work has demonstrated that the Plexin A1 receptor may also bind Slit (34).

A combination of in vitro and in vivo studies have led to a better understanding of the signaling cascades downstream of Robo receptors. Since Robos do not possess any intrinsic enzymatic activity, they depend on other binding partners to mediate their effects. Many members of the Robo complex are involved in regulating the function of Rho family GTPases such as RhoA, Rac1, and Cdc42 (35). These include Slit-Robo Rho Gtpase-activating proteins (SRGAPs), CrossGAP (CrGAP), and the adaptor protein Dock (36). Dock further recruits p21-activated kinase (PAK) and Son of sevenless (SOS) as additional Rac effectors (37). Changes in the activity of these small GTPases leads to reorganization of the actin cytoskeleton and growth cone collapse. Robo receptors are also targets of phosphorylation. Sites within the CC0 and CC1 domain of Robos can be phosphorylated by the kinase Abl, inhibiting Slit-Robo signaling (38). Finally, the actin-associated proteins Ena/VASP and Adenylyl cyclase-associated protein 1 (CAP1) bind Robos and further mediate cytoskeletal reorganization (39).

Robos receptors also participate in homo- and heterodimeric interactions in vitro (40,41). Dimerization is mediated through binding between ectodomains (16). However, Slit binding does not appear to be dependent on receptor dimerization and the determination of the precise importance of multimeric Robo complexes awaits further in vivo studies (42).

Many questions remain about the regulation of Roundabout signaling in the growth cone. It is worthy to note that second messenger signaling events impact neuronal migration. Classic studies have shown that altering the levels of cyclic nucleotides and calcium in the growth cone can interfere with axon guidance signals (43,44). For example, increasing the ratio of cAMP/cGMP can switch the action of guidance molecules from neuronal repulsion to attraction (45). Added to this, it has been demonstrated that elevation of intracellular cAMP and the subsequent activation of PKA can suppress Robo signaling (46). Activation of Robo receptors triggers the release of calcium from intracellular stores (47). Inhibition of calcium release does not prevent growth cone collapse, but does interfere with the subsequent reversal in the direction of migration.

Thus, although it has been clearly demonstrated that Robo receptors interface with second messenger pathways, the mechanisms for ensuring precise regulation of this process are not fully understood. A growing body of work suggests that scaffolding proteins may function to recruit additional signaling enzymes to receptors and cellular locations important for axonal migration (48).

For example, 14-3-3 proteins have been shown to regulate PKA activity during growth cone turning (49). The scaffolding protein WAVE1 is also expressed at the leading edge of growth cones, where it controls actin dynamics to facilitate axonal protrusions (50-53). Finally, the Drosophila anchoring protein Nervy coordinates signaling at the Plexin family of Semaphorin receptors (54). Plexins are an additional family of guidance receptors that have been implicated in growth cone repulsion and the promotion of dendritic arborization (55). Nervy is purported to cluster PKA at the Plexin receptor, thereby facilitating the termination of Semaphorin signaling through the phosphorylation of these receptors (54). Taken together, these studies provide a precedent for the notion that scaffolding proteins govern dynamic aspects of neuronal guidance and development.

WAVE1 and Nervy are both members of a class of protein scaffolds known as A-kinase anchoring proteins (AKAPs). A-kinase anchoring proteins (AKAPs) were first identified by their ability to bind the regulatory subunits of protein kinase A (56). Subsequent work has shown that AKAPs are capable of assembling complexes containing PKA and other signaling molecules at specific receptors and subcellular regions (57). By scaffolding these enzymes near both upstream activators and downstream targets, they provide both enhanced specificity and sensitivity to numerous signaling pathways.

The data presented here provides the first evidence that AKAP-associated enzymes may regulate Robo receptors. We propose that the interaction of AKAP79/150 with Robos may position PKC for a role in the fine-tuning of axonal and dendritic guidance. In addition, we present evidence that 14-3-3 proteins also complex with Robo receptors. The interaction of scaffolds with only specific members of the Robo family may contribute to signaling differences between receptors. Hence, scaffold-mediated modulation of Roundabout signaling may provide enhanced regulation of neuronal guidance.

Chapter 2: AKAP79/150 interacts with Robo2 and Robo3

Introduction:

One of the best studied neuronal scaffolds is AKAP79/150 (note: AKAP79 is the human form and AKAP150 is the murine ortholog). This anchoring protein localizes protein kinase A (PKA), protein kinase C (PKC), and the phosphatase calcineurin to the postsynaptic density (58). AKAP79/150 tethers these enzymes to a number of neuronal receptors to provide enhanced control of signal activation and termination. These include the α-amino-3-hydroxy-5-methylisooxazole-4-propionic acid (AMPA) and N-methyl D-aspartate (NMDA) families of glutamate receptors, L-type calcium channels, potassium channels, GABA receptors as well as a number of G protein-coupled receptors (59-62).

Anchored signaling through AKAP79/150 at AMPA and NMDA receptors in the hippocampus regulates changes in synaptic strength that are believed to underlie learning and memory (63). Long-term potentiation (LTP) and long-term depression (LTD) are two forms of synaptic plasticity commonly used to model memory storage in the hippocampus (64). Both of these processes are dependent on NMDA receptor activation. The subsequent modulation of synaptic strength is due to altered levels of extrasynaptic and synaptic AMPA receptors. High frequency stimulation, leading to significant levels of calcium entry through NMDA receptors, results in LTP and an increase in synaptic strength. The elevated calcium levels activate protein kinases such as PKA, PKC, and CamKII to phosphorylate AMPA receptors and stabilize their accumulation at the plasma

membrane. LTD results from low frequency stimulation that triggers persistent low levels of calcium entry. This instead activates the protein phosphatases calcineurin and PP1 to dephosphorylate AMPA receptors and promote their endocytosis.

The ability to precisely activate each of these pathways following NMDA receptor opening requires signaling enzymes to be assembled in proximity to the site of calcium entry. Numerous studies have demonstrated that scaffolds such as AKAP79/150 are essential to this process. For example, 8 week old mice expressing a form of AKAP150 unable to bind RII exhibit deficits in hippocampal LTP (65). Staining for RII in anchoring-deficient animals reveals that PKA is dramatically relocalized from dendritic spines into the dendritic shafts (66). These results demonstrate that AKAP150 is the predominant AKAP responsible for anchoring PKA at dendritic spines.

AKAP150 knockout animals also have impaired LTD (66,67). Furthermore, studies in mice specifically lacking the conserved PxIxIT region of AKAP150 also show LTD deficits (68,69). As the PxIxIT motif in AKAP150 is responsible for calcineurin binding, this suggests that phosphatase anchoring is required for functional LTD (70).

PKC anchoring through AKAP79/150 has likewise been shown to be important for the function of a number of receptors (71). For example, this anchoring

protein tethers PKC to M-channels (72). M-channels are a subtype of potassium channel involved in regulating membrane excitability. AKAP79/150-anchored PKC at the M-channel enhances suppression of channel conduction following muscarinic receptor activation.

Finally, AKAP79/150 is capable of complexing with numerous adenylyl cyclases. AC2,3,5,6, 8, and 9 have all been found to bind this anchoring protein (73). By bringing the enzymes responsible for cAMP production together with the cAMP-dependent protein kinase (PKA), AKAP79/150 ensures a rapid response to the production of this second messenger. In addition, AC8 is one of the calcium-stimulated cyclases, and is activated following localized calcium entry through NMDA receptors (74,75).

AC5 anchoring by AKAP79/150 also contributes to AMPA receptor regulation following activation of NMDA receptors. Loss of AC5 anchoring decreases AMPA receptor phosphorylation and leads to receptor internalization (76). This suggests that both kinase and AC anchoring through this AKAP are required for maintaining receptor phosphorylation. AKAP79/150-anchored PKA is also capable of phosphorylating ACs themselves, suppressing cAMP synthesis (77). Therefore, AKAP79/150 may both assemble an AC-kinase complex for rapid signal activation, but also participate in termination to maintain highly localized signaling domains.

Overall, these studies demonstrate that AKAP79/150 enhances regulation of neuronal receptors through the anchoring of a variety of signaling enzymes. AKAP79/150 complexes integrate second messenger signaling through calcium and cAMP to enhance crosstalk between pathways. The use of these same second messenger pathways by Roundabout receptors raises the question of whether scaffolds such as AKAP79/150 also contribute to the regulation of SLIT-Robo signaling.

Results:

Mass spectrometry identifies Robo2 as a putative AKAP79/150 binding partner*:* Previous work has shown that AKAP79/150 is a multifunctional anchoring protein that interacts with a range of neuronal binding partners (58,78-80). Therefore, we conducted a proteomic screen to look for additional proteins interacting with the murine ortholog, AKAP150. Protein complexes were immunoprecipitated from mouse brain extracts using a polyclonal antibody against AKAP150 and separated by SDS gel electrophoresis ((81); Fig. 1*A*, *lane 2*). Control immunoprecipitations were performed with IgG (Fig. 1*A*, *lane 1*). Silver stained bands that were enriched in the AKAP150 immunoprecipitation were excised and subjected to protein identification using MALDI-TOF mass spectrometry. Known members of the AKAP150 complex were detected, including the NR2A subunit of the NMDA receptor, thereby validating this approach (59,82-84). In addition, we identified several previously unknown AKAP150 binding partners (Fig. 1*B*). These included key elements of neuronal guidance pathways such as the Roundabout receptor Robo2 and its ligands Slit2

and Slit3 (2,5). These results imply that AKAP150 signaling complexes have the potential to interface with the axon guidance machinery and dendritic ion channels.

AKAP79 interacts with the Robo2 receptor: In order to validate the results from our proteomics screen, it was important to determine whether AKAP79/150 interacts with Robo2 inside cells. Therefore, HEK293 cells were transfected with plasmids encoding FLAG-tagged AKAP79, the human ortholog of the anchoring protein, and V5-tagged Robo2. Cells were harvested after 48 hours and cell lysates were subjected to immunoprecipitation with anti-FLAG antibody. Western blot analysis of AKAP79 immune complexes detected the Robo2 receptor (Fig. 1*C*, *top panel*, *lane 1*). Control experiments performed from cells transfected with only Robo2 plasmid were negative (Fig. 1*C*, *top panel*, *lane 2*). Immunoblot analysis evaluated the expression levels of both proteins in HEK293 cell lysates (Fig. 1*C*, *bottom two panels*). Further validation of this protein-protein interaction was provided by reciprocal immunoprecipitation experiments. Immunoblots revealed the presence of AKAP79 in Robo2 immune complexes, but not control immunoprecipitations (Fig. 1*D*, *top panel*). Immunoblot analyses evaluated the expression levels of both proteins in HEK293 cell lysates (Fig. 1*D*, *bottom two panels*). Collectively, these results allow us to conclude that heterologously expressed AKAP79 and Robo2 interact in HEK293 cells.

Immunofluorescence staining further suggests that Robo2 and AKAP79 reside in the same subcellular compartment (Fig. 1, *E*-*G*). Confocal imaging revealed that recombinant AKAP79 (Fig. 1*E*, *red*) and Robo2 (Fig. 1*F*, *green*) have overlapping regions of expression and accumulate near the plasma membrane in HEK293 cells. This is best observed in the composite image of the merged signals (Fig. 1*G*). These results imply that AKAP79 and Robo2 co-distribute inside cells.

Robo2 is expressed throughout the developing murine hippocampus, a region of the brain that is enriched with AKAP79/150 (7,66). Thus, a more pertinent validation of the interaction between these two proteins was to be found in primary cultures of mouse hippocampal neurons grown for 15 days *in vitro* (DIV 15). Endogenous AKAP150 (Fig. 1, *H* and *J*, *red*) was found to overlap with recombinant Robo (Fig. 1, *I* and *J*, *green*). Higher magnification confocal images reveal that both proteins accumulate at the tips of neuronal processes (Fig. 1, *K*-*M, arrows*). Further experiments revealed that endogenous AKAP150 (Fig. 1, *N* and *P*, *red*) co-distributed with endogenous Robo2 (Fig. 1, *O* and *P*, *green*) in discrete clusters. These regions of signal overlap were located in both the cell body and dendrites of mouse hippocampal neurons that had been cultured for 4 days. At higher magnification, it was evident that both proteins co-clustered at the tips of neuronal processes, including putative dendritic growth cones (Fig. 1, *Q*-*V*).

Figure 1

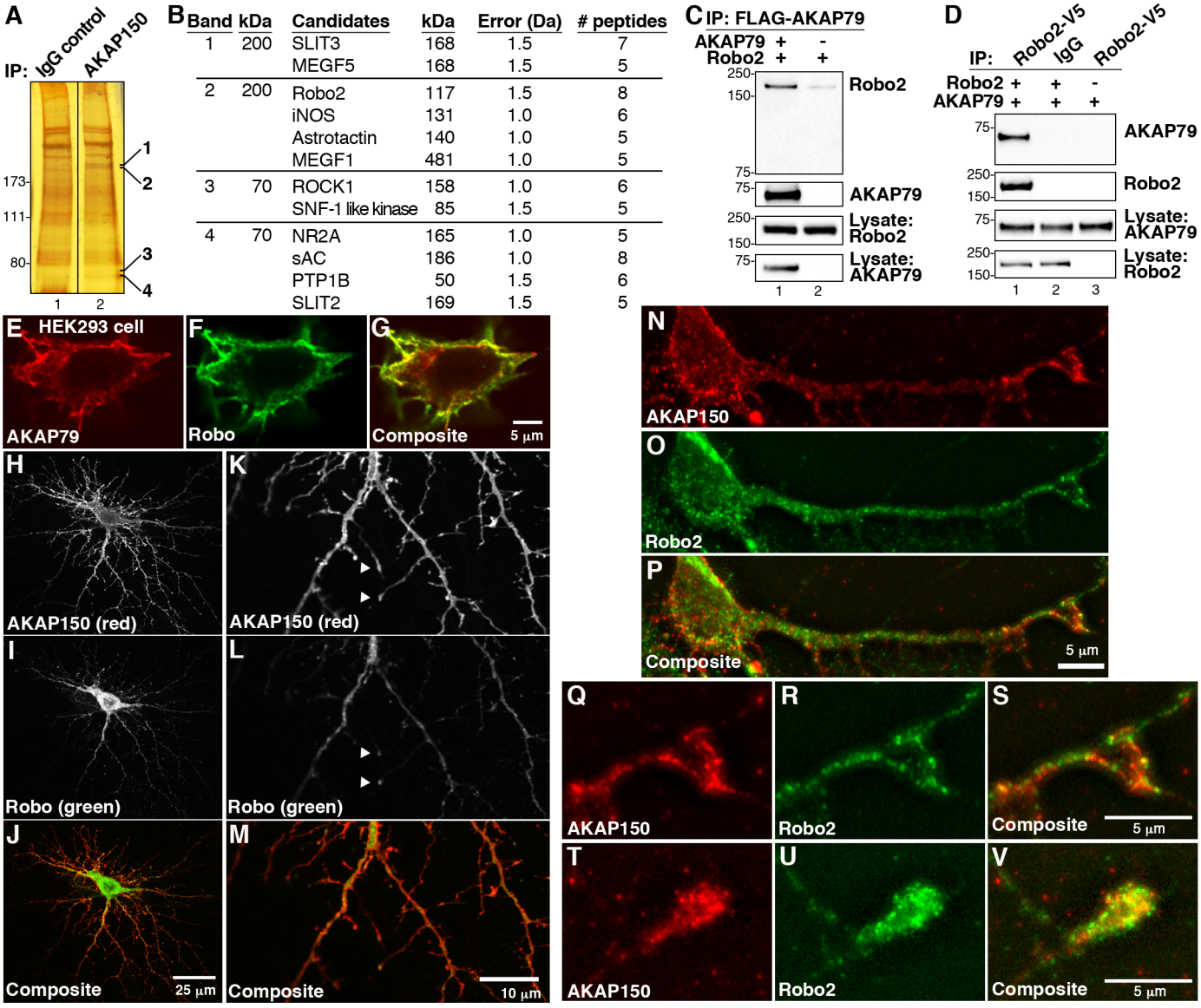
A
IP: IgG control
AKAP150
173
111
80
1
2
3
4
B
Band kDa Candidates kDa Error (Da) # peptides
1 200 SLIT3 168 1.5 7
MEGF5 168 1.5 5
2 200 Robo2 117 1.5 8
iNOS 131 1.0 6
Astrotactin 140 1.0 5
MEGF1 481 1.0 5
3 70 ROCK1 158 1.0 6
SNF-1 like kinase 85 1.5 5
4 70 NR2A 165 1.0 5
sAC 186 1.0 8
PTP1B 50 1.5 6
SLIT2 169 1.5 5
C IP: FLAG-AKAP79
AKAP79 + -
Robo2 + +
250
150
75
Robo2
AKAP79
Lysate: Robo2
Lysate: AKAP79
1 2
D
IP: Robo2-V5 IgG Robo2-V5
Robo2 + + -
AKAP79 + + +
75
AKAP79
250
150
Robo2
Lysate: AKAP79
Lysate: Robo2
1 2 3
E HEK293 cell
AKAP79
F
Robo
G
Composite
5 µm
H
AKAP150 (red)
K
AKAP150 (red)
I
Robo (green)
L
Robo (green)
J
Composite
25 µm
M
Composite
10 µm
N
AKAP150
O
Robo2
P
Composite
5 µm
Q
AKAP150
R
Robo2
S
Composite
5 µm
T
AKAP150
U
Robo2
V
Composite
5 µm

Figure 1. **AKAP79/150 interacts with Robo2**. *A*, mass spectrometry screening to identify AKAP150 binding proteins. Immune complex complexes were isolated from mouse brain lysates. Silver stained SDS-PAGE gels of control (*lane 1*) and AKAP150 (*lane 2*) immune complexes. Molecular weight markers are indicated. Bands present in AKAP150 immunoprecipitations were excised (*bands indicated*) and protein determination was by MALDI-TOF mass spectrometry. *B*, table of proteins identified in AKAP150 complexes. Columns indicate the name, molecular weight, mass error, number of peptides detected, and percent coverage of each protein. *C and D*, validation of AKAP150 association with Robo2. HEK293 cells were transfected with FLAG-AKAP79 and V5-Robo2. FLAG immune complexes were immunoblotted for Robo2 (*top*) and AKAP79 (*upper middle*). Loading controls for Robo2 (*lower middle*) and AKAP79 (*bottom*) are included. *D*, reciprocal immunoprecipitation of Robo2 immune complexes blotted for AKAP79 *(top)* and Robo2 *(upper middle)*. *E-G*, confocal imaging of AKAP79 (*E and G, red*) and Robo (*F and G, green*) in HEK293 cells. *H-P***,** DIV 15 mouse hippocampal neurons were transfected with Robo and immuno-stained for Robo and endogenous AKAP150. The staining patterns of AKAP150 (*H* and *K, grayscale* and *J* and *M, red)* and Robo (*I* and *L, grayscale* and *J* and *M, green*) were assessed by confocal microscopy. Details of the dendritic arbor are shown at higher magnification, and co-distribution of AKAP150 and Robo at tips of neuronal processes is indicated with arrows *(K-M)*. *N-P***,** neonatal mouse hippocampal neurons cultured for 4 DIV were stained for endogenous AKAP150 (*N* and *P, red*) and endogenous Robo2 (*O* and *P, green)*. The staining patterns of both proteins were assessed by digital-deconvolution microscopy. *Q-V,* higher magnification images of dendritic processes showing co-clustering (*yellow*) of AKAP150 (*Q*, *S*, *T*, *V, red*) and Robo2 (*R*, *S*, *U*, *V, green*) in putative growth cones.

Mapping the AKAP79-Robo2 binding interface: On the basis of mass spectrometry identification and biochemical analyses, we postulate that AKAP79/150 and Robo2 can exist as a macromolecular complex. The next phase of these studies was to determine what regions of AKAP79 and Robo2 participate in this protein-protein interaction. To map the Robo2 binding site on AKAP79, we split the anchoring protein into amino-terminal (residues 1-153), central (residues 154-296), and carboxyl-terminal (residues 297-427) fragments. Each AKAP79 fragment was expressed as a GST fusion protein (Fig. 2*A*, *middle panel*). This family of deletion fragments was used to pull down Robo2 from HEK293 cell lysates. Immunoblot analysis revealed that Robo2 selectively bound to the amino-terminal fragment of AKAP79, suggesting that its principal binding site lies between residues 1-153 of the anchoring protein (Fig. 2*A*, *top panel*, *lane 2*). It should be noted that Robo2 weakly interacted with the carboxyl terminal regions of the anchoring protein (Fig. 2*A*, *top panel*, *lane 4*). Control experiments confirmed that equivalent amounts of Robo2 were used in all binding experiments (Fig. 2*A*, *bottom panel*). These experiments suggest that multiple regions of AKAP79 may interface with Robo2.

In reciprocal experiments, a similar approach was used to map the region of Robo2 that binds to the anchoring protein. The cytoplasmic tail of Robo2 was split into three fragments (Fig. 2*B*, *middle panel*). These GST-fusion proteins were then used to pull down FLAG-AKAP79 from HEK293 cell lysate. The anchoring protein bound strongly to a central portion of Robo2 that encompasses

residues 991-1141 (Fig. 2*B*, *top panel*, *lane 3*), although weaker binding of AKAP79 was also detected to a fragment of Robo2 that is immediately proximal to the membrane-spanning segment (residues 881 to 990; Fig. 2*B*, *top panel*, *lane 2*). This led us to conclude that the primary AKAP79 binding site lies between residues 991-1141 of Robo2. Control experiments confirmed that equivalent amounts of AKAP79 were used in all binding experiments (Fig. 2*B*, *bottom panel*).

To further narrow down the AKAP79 binding sites, we generated an additional family of truncations in the cytoplasmic tail of Robo2 (Fig. 2*C*). AKAP79 binding was analyzed as described above. These studies revealed that a Robo2 receptor expressing the first 1070 residues was still competent to bind AKAP79. This represents a region of approximately 190 residues that reside in the cytoplasm of cells (Fig. 2*C*). Further truncation of the cytoplasmic tail of Robo2 prevented interaction with the anchoring protein (Fig. 2*D*, *top panel*, *lane 5*). Thus, we can conclude that residues 991-1070 of Robo2 are necessary for interaction with AKAP79. Control experiments confirmed that equivalent amounts of Robo2 and AKAP79 were used in all binding experiments (Fig. 2*D*, *middle* and *bottom panels*).

AKAP79/150 binds directly to the cytoplasmic tails of Robo2 and Robo3*:* Studies in the previous sections indicate that human AKAP79 and its murine ortholog AKAP150 have the capacity to interact with Robo2. Next, we

investigated whether Robo2 is capable of interacting with endogenous AKAP150 and its anchored enzymes. A GST-tagged Robo2 881-1378 fragment was used to perform pull-downs from mouse brain lysate. Overlay with labeled RII revealed that an AKAP of the molecular weight of AKAP150 was bound to this Robo2 fragment (Fig. 2*E*, *upper panel*, *lane 2*). Western blotting confirmed that this band corresponded to endogenous AKAP150 (Fig. 2*E*, *top panel*, *lane 2*). The anchoring protein was not detected in control pull-downs using GST alone (Fig. 2*E*, *top two panels*, *lane 1*). Analysis of mouse brain lysates verified that equivalent amounts of AKAP150 were present in both samples (Fig. 2*E*, *lower two panels*). Related experiments established that the AKAP79/150 binding partners RIIα, the phosphatase PP2B (B subunit), and conventional PKCs co-purify with the Robo2 881-1378 fragment (Fig. 2*F*, *top three panels*, *lane 2*). Collectively, these findings strengthen our view that Robo2 associates with AKAP150 complexes containing a range of anchored signaling enzymes. Additional experiments revealed that GST-Robo2 also binds human AKAP79 from HEK293 cell lysates (Fig. 2*G*, *top panel*, *lane 4*).

AKAP79/150 binds directly to certain membrane proteins, such as the L-type calcium channel and the KCNQ2 subunits of the M-channel (60,66,80,85-87). In contrast, NMDA and AMPA receptors interact with AKAP79/150 through a bridging interaction with membrane-associated guanylate kinase (MAGUK) proteins (59,71,82). To determine if AKAP79 can interface directly with Robo2, we repeated our GST-Robo2 pull-downs using His-tagged AKAP79 purified from

E. coli. These experiments confirmed that AKAP79 binds directly to Robo2, without the need for an adaptor protein (Fig. 2*H*, *top panel*, *lane 4*). Purified recombinant RII was used as a negative control for these binding studies (Fig. 2*H*, *bottom panel*, *lane 2*).

There are four members of the Robo family of chemotactic guidance receptors (27). Therefore, it seemed logical to explore the possibility that AKAP79/150 may associate with other Robo receptor isoforms. However, only Robo1, 2, and 3 are expressed in neurons (27). Therefore, AKAP79 pull-down experiments were conducted with GST-fusion proteins encompassing the cytoplasmic tails of Robo1, Robo2, and Robo3. These binding studies revealed that Robo3 also associates with AKAP79 (Fig. 2*I*, *top panel*, *lane 4*). GST-Robo2 binding to AKAP79 served as an internal control (Fig. 2*I*, *top panel*, *lane 3*). Immunoblot analysis confirmed that equivalent amounts of each binding partner were present in these experiments (Fig. 2*I*, *middle* and *lower panels*). Sequence homology between Robo2 and Robo3 within the region that spans the AKAP binding site may explain why the AKAP is capable of binding both of these receptors. In contrast, the Robo1 isoform contains an insertion within this region, potentially explaining why it does not associate with this anchoring protein (Fig. 2*I*, *top panel*, *lane 2*).

Figure 2

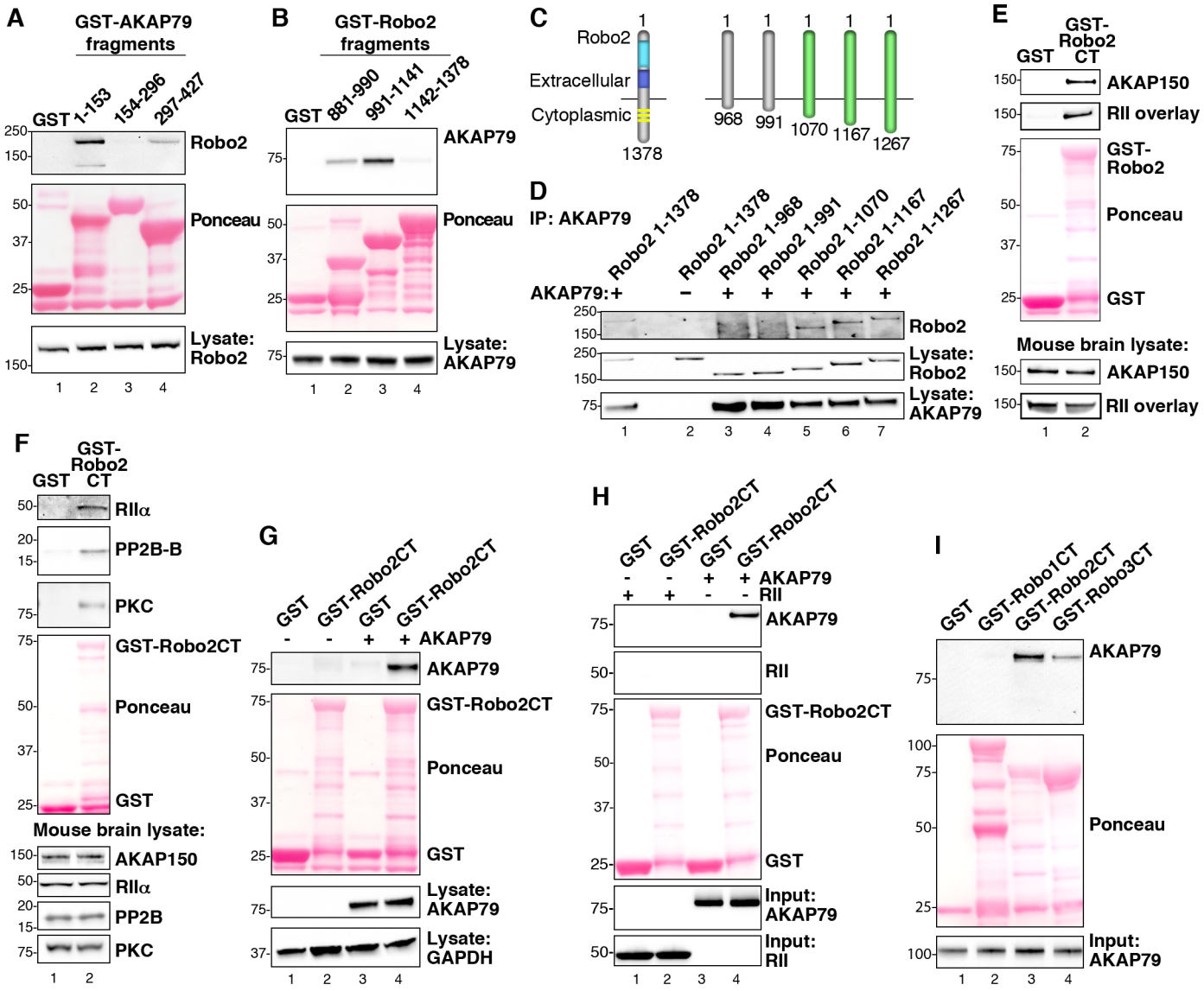
A
GST-AKAP79 fragments
GST
1-153
154-296
297-427
Robo2
Ponceau
Lysate: Robo2
B
GST-Robo2 fragments
GST
881-990
991-1141
1142-1378
AKAP79
Ponceau
Lysate: AKAP79
C
Robo2
Extracellular
Cytoplasmic
1
968
991
1070
1167
1267
1378
D
IP: AKAP79
Robo2 1-1378
Robo2 1-968
Robo2 1-991
Robo2 1-1070
Robo2 1-1167
Robo2 1-1267
AKAP79:+ − + + + + +
Robo2
Lysate: Robo2
Lysate: AKAP79
E
GST-Robo2 CT
GST
AKAP150
RII overlay
GST-Robo2
Ponceau
GST
Mouse brain lysate:
AKAP150
RII overlay
F
GST-Robo2 CT
GST
RIIα
PP2B-B
PKC
GST-Robo2CT
Ponceau
GST
Mouse brain lysate:
AKAP150
RIIα
PP2B
PKC
G
GST
GST-Robo2CT
GST
GST-Robo2CT
AKAP79
AKAP79
GST-Robo2CT
Ponceau
GST
Lysate: AKAP79
Lysate: GAPDH
H
GST
GST-Robo2CT
GST
GST-Robo2CT
AKAP79
RII
AKAP79
RII
GST-Robo2CT
Ponceau
GST
Input: AKAP79
Input: RII
I
GST
GST-Robo1CT
GST-Robo2CT
GST-Robo3CT
AKAP79
Ponceau
Input: AKAP79

Figure 2. **Biochemical characterization of the Robo2-AKAP79/150 interaction.** *A*, purified GST-AKAP79 fragments containing GST alone (*lane 1*), aa1-153 (*lane 2*), 154-296 (*lane 3*), and 297-427(*lane 4*) were used to isolate Robo2 from HEK293 cell lysates. Molecular weight markers are indicated. *B*, GST-tagged fragments including GST alone (*lane 1*), aa 881-990 of Robo2 (*lane2*), 991-1141 of Robo2 (*lane3*), and 1142-1378 of Robo2 (*lane 4*) were used to pull down overexpressed AKAP79 from HEK293 cell lysates. *C*, diagram depicting progressive truncation of the Robo2 receptor used for fine mapping of the AKAP79 binding site. The first and last residues of each fragment are denoted. *D*, AKAP79 and truncated Robo2 receptors were overexpressed in HEK293 cells. AKAP79 immune complexes were immunoprecipitated and Robo2 binding was assessed by immunoblot. *E*, purified Robo2 C-terminus (*Robo2-CT*) fused to GST was incubated with mouse brain lysate. Immunoblots were probed for AKAP150 (*top*) and overlaid with digoxigenin-labeled RII (*upper middle*). *F*, GST-Robo2CT pull-downs from mouse brain lysate were immunoblotted for RIIa *(top*), PP2B (*second from top*), and PKC (*third from top*). *G*, GST-Robo2CT pull-downs from HEK293 cell lysate containing overexpressed AKAP79 were probed for AKAP79 (top). *H*, GST-Robo2CT was incubated with either purified His-AKAP79 or His-RII. GST-Robo2CT complexes were immunoblotted for AKAP79 (*top*) and RII (*upper middle*). *I*, the C-termini of Robo1, Robo2 and Robo3 were each fused to GST and purified from bacteria. Purified His-AKAP79 was incubated with the GST-RoboCT proteins and immunoblots of the GST-Robo complexes were probed for AKAP79 (*top*).

Much of the knowledge of Roundabout receptors has been gleaned from the investigation of axonal guidance in the developing spinal cord. Signals processed by Robo1 and Robo2 expel axons from the floor plate of the spinal cord and prevent inappropriate recrossing of the midline (11). In contrast, signaling through Robo3 promotes midline crossing (13). Therefore, we reasoned that association with AKAP150 might influence aspects of axonal guidance in mouse spinal commissural axons. As a prelude to these studies, we examined whether AKAP150 is expressed in the developing spinal cord of E11.5 mice. Immunostaining revealed that AKAP150 is broadly expressed throughout the developing spinal cord (Fig. 3*A*, *green*). In keeping with published reports, Robo2 expression was restricted to the ventral and lateral funiculi ((10); Fig. 3, *B* and *C*, *red*). These two regions of the spinal cord were re-examined at higher magnification by confocal microscopy (Fig. 3, *D-J*). Co-distribution of both signals was most apparent in the ventral and lateral funiculi (Fig. 3, *D-F*, *yellow*), but some overlap of staining was also observed in the cell bodies of commissural neurons (Fig. 3, *H-J*, *yellow*). Control experiments using the same antibodies confirmed that the AKAP150 signal was absent in equivalent sections from E11.5 AKAP150 -/- mice ((66) Fig. 3, *K*, *N*, and *Q*). Robo2 staining appeared normal in these sections (Fig. 3, *L-P*). Normal patterns of midline crossing were observed when wildtype and AKAP150 -/- sections were stained for neural cell adhesion molecule L1, a post-crossing axonal marker ((88); Fig. 3, *T* and *U*). Thus, it would appear that although AKAP150 and Robo2 are co-distributed in the developing

spinal cord, their association does not influence midline crossing of spinal commissural axons in mouse embryos.

Figure 3

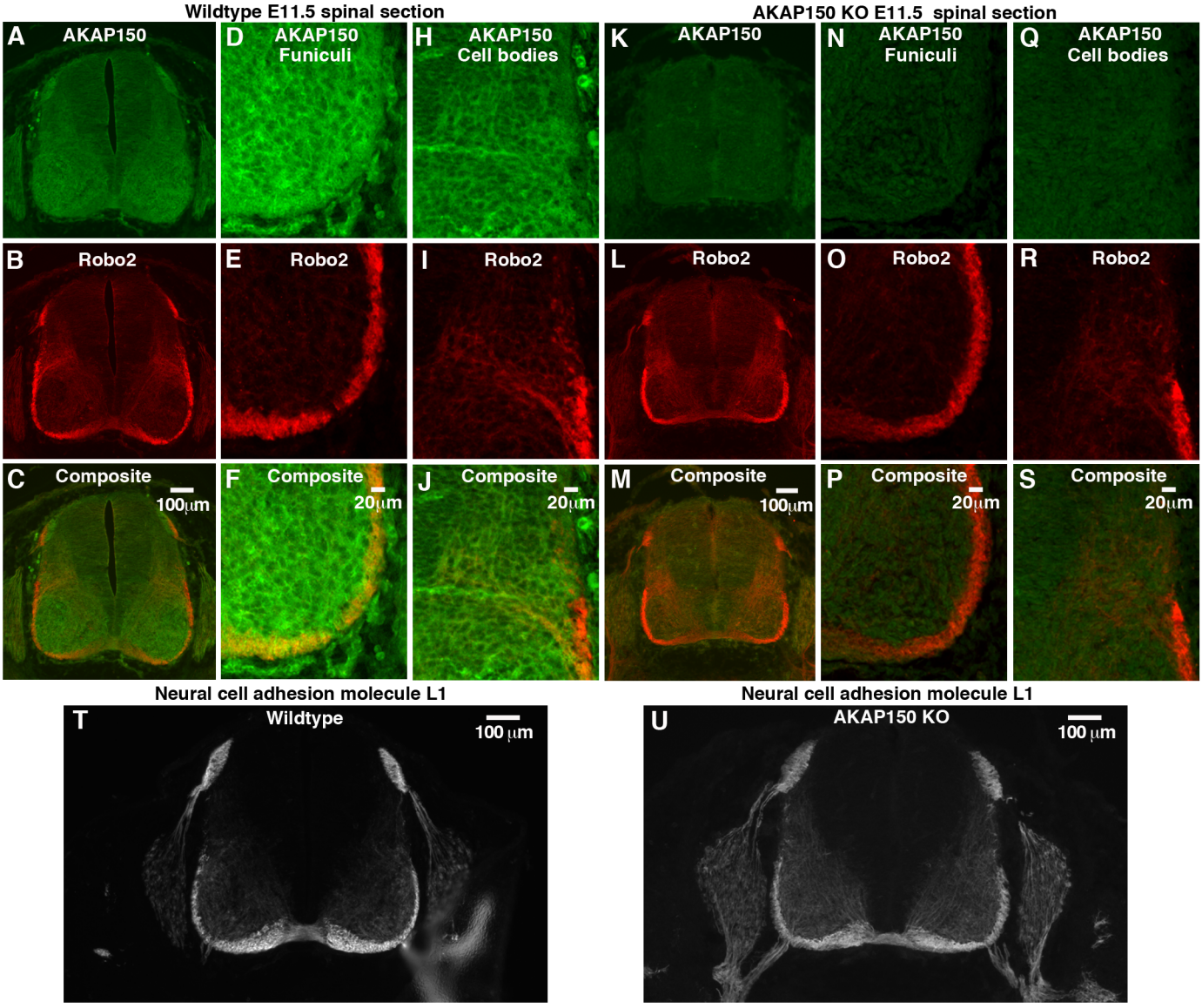
Wildtype E11.5 spinal section
AKAP150 KO E11.5 spinal section
A AKAP150
D AKAP150 Funiculi
H AKAP150 Cell bodies
K AKAP150
N AKAP150 Funiculi
Q AKAP150 Cell bodies
B Robo2
E Robo2
I Robo2
L Robo2
O Robo2
R Robo2
C Composite 100μm
F Composite 20μm
J Composite 20μm
M Composite 100μm
P Composite 20μm
S Composite 20μm
Neural cell adhesion molecule L1
T Wildtype 100 μm
Neural cell adhesion molecule L1
U AKAP150 KO 100 μm

Figure 3. **AKAP150 is expressed in the developing spinal cord where it co-distributes with Robo2 in specialized regions**. Transverse sections of E11.5 spinal cords from wildtype and AKAP150 -/- mice were stained for AKAP150 and Robo2, and imaged using widefield fluorescence microscopy *(wildtype; A-C and AKAP150 -/-; K-M)*. AKAP150 is shown in green and Robo2 is shown in red. Higher magnification spinning disc confocal images provide more detailed localization of these proteins in the funiculi (*wildtype; D-F* and *AKAP150 -/- N-P*) and commissural neuron cell bodies (*wildtype; H-J* and *AKAP150 -/-; Q-S*). *T* and *U,* Sections of spinal cord from wildtype (*T*) and AKAP150 -/- mice (*U*) stained for neural cell adhesion molecule L1, a marker for midline crossing.

Robo2 and Robo3 co-distribute with AKAP150 in the adult mouse brain:

Robo receptors are expressed in the adult brain (23). Likewise, neuronal AKAP150 expression peaks later in development (83). Therefore, we wondered if AKAP150 co-distributed with Robo receptors in the brains of mature mice. To test this possibility, brains from 4-month-old wildtype and AKAP150 -/- mice were isolated and paraffin embedded. Sagittal sections were prepared and immunofluorescent staining with antibodies to AKAP150, Robo2, and Robo3 was completed. Fluorescent microscopy of intact sagittal sections at low magnification revealed distinct but overlapping staining patterns for AKAP150 and Robo2 and Robo3 in a variety of brain regions (data not shown). Widefield fluorescent images (40× objective) show overlapping expression patterns for AKAP150 (*red*) with both Roundabout receptors (*green*) in hippocampal sections (Fig. 4, *A* and *E*). Upon higher magnification (63×) analysis on a confocal microscope, the co-distribution of the anchoring protein with Robo2 (Fig. 4, *B-D*) and Robo3 (Fig. 4, *F-H*) was evident in the CA1 region of the hippocampus. Likewise, analysis of lower magnification images detected both Roundabout receptors co-distributed with AKAP150 in the islands of calleja in the olfactory tubercle (Fig. 4, *I* and *M*, *yellow*). Overlapping staining patterns between AKAP150 and both Robo2 and Robo3 were also evident in this same tissue at higher magnification (Fig. 4, *J-L* and *N-P*). Staining patterns of Robo2 and Robo3 were unchanged in brain sections from AKAP150 -/- mice (data not shown).

Figure 4

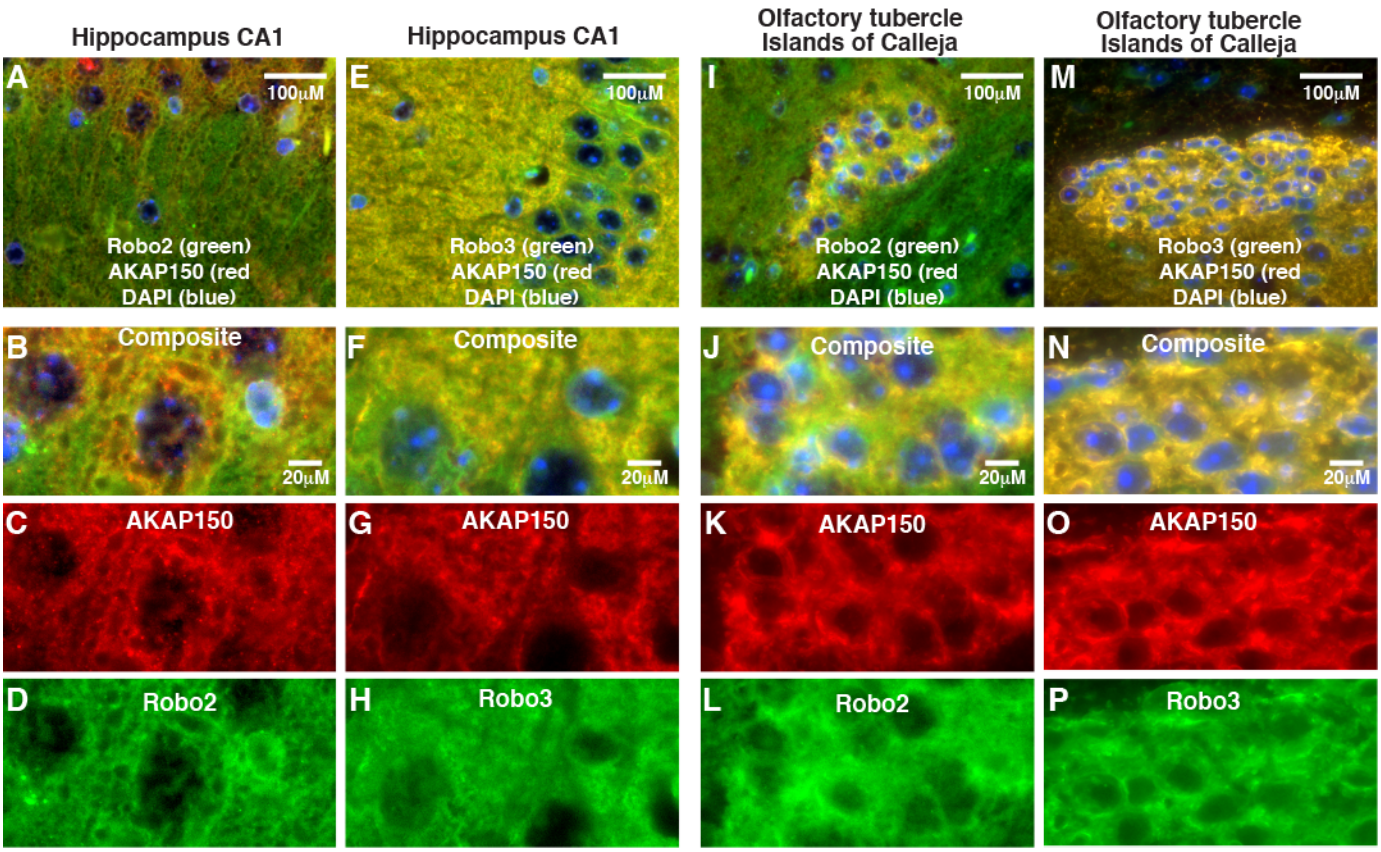
Hippocampus CA1
Hippocampus CA1
Olfactory tubercle Islands of Calleja
Olfactory tubercle Islands of Calleja
A
100μM
Robo2 (green)
AKAP150 (red
DAPI (blue)
E
100μM
Robo3 (green)
AKAP150 (red
DAPI (blue)
I
100μM
Robo2 (green)
AKAP150 (red
DAPI (blue)
M
100μM
Robo3 (green)
AKAP150 (red
DAPI (blue)
B
Composite
20μM
F
Composite
20μM
J
Composite
20μM
N
Composite
20μM
C
AKAP150
G
AKAP150
K
AKAP150
O
AKAP150
D
Robo2
H
Robo3
L
Robo2
P
Robo3

Figure 4. **AKAP150 co-distributes with Robo2 and Robo3 in the adult brain**. Sagittal paraffin-embedded sections from 16 week old mouse brains were immunostained for AKAP150 (*A-C, E-G, I-K, M-O, red*) and either Robo2 (*A, B, D, I, J, L, green*) or Robo3 (*E, F, H, M, N, O, green*). *A-H,* staining in the CA1 region of the hippocampus. *I-P,* staining of the islands of calleja in the olfactory tubercle. Images from top panel were collected at low magnification, while lower panels represent high magnification confocal images from same region.

Discussion:

Our findings demonstrate that AKAP79/150 binds to Robo2 and Robo3, localizing signaling molecules to these receptors. However, it is unknown how AKAP-anchored enzymes might regulate Robo function. One possibility is through modulating crosstalk between Robo receptors and other signaling pathways. Work from the Raper lab has demonstrated that the cytokine SDF-1 is capable of inhibiting axonal repulsion mediated by Slit-Robo signaling (46,89). SDF-1 binding to the CXCR4 receptor activates a number of downstream effectors, including PKA. Interestingly, PKA appears to be required for SDF-1 silencing of SLIT-Robo signaling. The particular PKA targets involved in this process have not been comprehensively investigated, but preliminary evidence using specific inhibitors of small GTPases suggests that this effect is at least partially due to the phosphorylation and subsequent inactivation of Rho.

Furthermore, the sensitivity of Robo signaling to SDF-1 is dependent on the calcium-sensitive adenylyl cyclase AC8 (90). Loss of AC8 renders axons insensitive to SDF-1-mediated silencing of SLIT-Robo signaling. In zebrafish, this results in axons aberrantly failing to crossing the midline. As AKAP79/150 binds both PKA and AC8, it is possible that localization of these enzymes to Robo receptors may be important for ensuring sensitivity to SDF-1 inhibition. By tethering the signaling machinery responsible for cAMP production in proximity to PKA, this scaffold may promote rapid but highly specific crosstalk with the SDF-1/CXCR4 pathway.

In addition, the activation of many axon guidance receptors triggers a release of intracellular calcium, which can in turn modulate cAMP levels in the growth cone. The extent of calcium release alters the equilibrium of kinase and phosphatase activity in the developing axon (91). High levels of calcium result in the preferential activation of kinases and triggers axonal protrusion. Lower levels of calcium promote phosphatase activity and lead to growth cone collapse and axonal repulsion. This balance of kinase and phosphatase activation is reminiscent of the opposing regulation of LTD and LTP in the hippocampus. Just as AKAP79/150 is able to scaffold kinases and phosphatases to provide bi-directional control of synaptic plasticity, this AKAP may also serve a similar function during axonal and dendritic development.

There is already some evidence that the calcium-activated protein phosphatase calcineurin functions downstream of Robo receptors. Inhibition of calcineurin blocks SLIT-induced reorganization of the actin cytoskeleton in migrating olfactory ensheathing cells (47). Calcineurin appears to activate cofilin, removing a phosphate at serine 3 and stimulating actin depolymerization.

While this is currently no evidence implicating PKC as a downstream effector of Robo signaling, many second messengers produced following receptor activation are also capable of activating this kinase. Firstly, SLIT binding triggers elevations in intracellular calcium, an activator of PKC. This SLIT-induced release of

calcium from intracellular stores has been shown to be dependent on IP3 receptors. As production of IP3 also generates the PKC activator diacylglycerol, AKAP79/150-anchored PKC localized to Robo receptors would be positioned for rapid activation following SLIT binding.

Potential targets for AKAP79/150-anchored kinases include numerous Robo binding proteins, as well as the receptors themselves. Currently, Abl and Src are the only kinases known to phosphorylate the Robo family. However, many receptors that bind AKAP79/150 are direct targets of phosphorylation by anchored kinases. Determining whether Robos contain additional phosphorylation sites may yield insights into the regulation of these receptors.

Our results demonstrating co-distribution between AKAP79/150 and Robo receptors in hippocampal neurons suggests a potential role for AKAP regulation of Slit-Robo signaling in this brain region. Data from figure 1 raises the possibility that AKAP79/150 may regulate Robo2 signaling in the dendritic growth cones of neonatal hippocampal neurons. As Roundabout signaling has been found to control the development of dendritic arbors, it may be worth investigating whether this process is perturbed in AKAP150 -/- animals.

In addition, we observe co-expression of AKAP79/150 with Robo2 and Robo3 in multiple regions of the adult brain. These include the hippocampus, striatum, and olfactory tubercle. Previous work also supports expression of Robo receptors in

mature animals . However, post-developmental roles for Slit-Robo signaling are currently unknown.

A potential clue may be found in recent work on the function of the DCC receptor in adult mice. This receptor for the attractive guidance cue netrin regulates axon guidance during development. New data suggests that DCC is also expressed in the postsynaptic densities of mature neurons, where it helps to mediate changes in synaptic plasticity (92). Future experiments may be able to determine whether Slit-Robo signaling is likewise involved in the regulation of synaptic plasticity. As AKAP79/150 already is known to provide precise control over signaling in the PSD, Robo receptors may represent additional targets of AKAP-anchored enzymes in this subcellular location.

Chapter 3: AKAP79 enhances PKC phosphorylation of Robo3.1

Introduction:

Vertebrate Robo3 occupies a unique role within the Roundabout family. First, it is unable to bind Slit ligands. Additionally, Robo3 does not mediate axonal repulsion, but instead silences signaling through Robo1 and Robo2 (13). It is expressed prior to midline crossing and blocks repulsive signaling to facilitate attraction to the floor plate. Postcrossing, Robo3-mediated silencing is immediately lost, and Robo1 and Robo2 are again capable of triggering axonal repulsion. Robo3 appears to accomplish this inhibition through unknown mechanisms that do not alter protein expression levels of other Robo receptors.

Recent work has shown that Robo3 may in fact actively promote axonal attraction following netrin activation of the DCC receptor (14). Robo3 can complex with DCC through an interface located between its CC2 and CC3 domains. DCC activation leads to phosphorylation of Robo3 at Y1019. Previous studies have suggested that tyrosine phosphorylation of other Robo receptors may inhibit repulsive signaling (38).

An explanation for how Robo3-mediated silencing is lost following midline crossing was provided by analyses of alternatively spliced Robo3 isoforms (19). The Robo3.1 isoform is expressed precrossing and functions to silence signaling through other Robos. Postcrossing axons instead express the Robo3.2 isoform. Robo3.2 is unable to inhibit other members of the Robo family, thus allowing Slit

repulsion to occur. These two isoforms differ only in their distal C-termini, with Robo3.1 containing a unique 78 amino acid arginine/serine rich region. It is clear that this region is required for Robo3's ability to silence SLIT-Robo signaling. However, it is unknown whether this is due to conformational changes in Robo3, differential interaction with binding partners, altered phosphorylation of the receptor itself, or other factors.

Results:

Robo3 is phosphorylated by anchored PKC: AKAP150 expression in the hippocampus peaks at postnatal day 14 in mice (83), a developmental stage when Robo receptors, their Slit ligands and other axon guidance molecules are also present in the hippocampus (10). For instance, the Netrin receptor Deleted in Colorectal Cancer is enriched in the postsynaptic density where it is required to facilitate long-term potentiation, an electrophysiological paradigm for learning and memory (92). Therefore, it seemed plausible that Robo receptors might contribute to acute neuronal signaling events that control synaptic strength. An attractive feature of this hypothesis is that AKAP79/150 signaling complexes also populate the postsynaptic density where they provide local control of synaptic strength (81,93). In keeping with this notion, deletion of AKAP150 in mice impairs long-term depression due to the loss of PKA, PKC, and PP2B anchoring (66,72,94).

In light of these findings, we performed in vitro kinase assays to determine if any Robo receptors are targets of AKAP150-anchored kinases. Purified GST-tagged

cytoplasmic tails of Robo1, Robo2, and Robo3 were immobilized on beads and phosphorylated in vitro with a mixture of conventional PKCs and [^{32}P] ATP. Autoradiography revealed that only Robo3 was phosphorylated by PKC (Fig. 5*A*, *top panel*, *lane 3*). Analogous experiments showed that Robo1 was phosphorylated by protein kinase A whereas Robo3 was labeled to a lesser extent (Fig 5*B*, *top panel*, *lane 2* and *8*). However, we were unable to recapitulate PKA phosphorylation of either Robo receptor inside cells. Since Slit-Robo signaling can mobilize intracellular calcium (47), we reasoned that the selective phosphorylation of Robo3 by PKC might contribute to the unique function of this receptor. For these reasons, we focused on investigating PKC phosphorylation of Robo3.

Next, we performed experiments in the presence of AKAP79 to investigate the role of the anchoring protein in this phosphorylation event. Formation of a Robo3-AKAP79-PKC ternary complex enhanced phosphorylation of the substrate (Fig. 5*C*, *top panel*, *lane 2*) as compared to experiments performed in the absence of the anchoring protein (Fig. 5*C*, *top panel*, *lane 1*). This suggests that AKAP79-anchored PKC preferentially phosphorylates Robo3. A more stringent validation of this concept was performed in HEK293 cells as they express high levels of endogenous AKAP79. Cells were transfected with plasmids encoding full length V5 tagged-Robo3 and PKC activity was stimulated upon application of phorbol 12,13-dibutyrate (PDBu). Robo3 immune complexes were probed with an antibody that detects phosphorylated PKC substrates. Immunoblot analysis

revealed robust phorbol ester-dependent phosphorylation of Robo3 (Fig. 5*D*, *top panel*, *lane 2*) as compared to unstimulated controls (Fig. 5*D*, *top panel*, *lane 1*). Immunoblot analysis of whole cell lysates using the phospho-PKC substrates antibody confirmed kinase activation, and additional controls established that equivalent levels of Robo3 were present in each sample (Fig. 5*D*, *middle* and *bottom panels*).

We subsequently probed a family of Robo3 truncation fragments in an attempt to locate the sites of PKC phosphorylation. These mapping studies indicate that the extreme carboxyl terminus of Robo3 (residues 1236-1386) contained the site(s) of PKC phosphorylation (Fig. 5*E*, *top panel*, *lane 2*). This region of the Robo3 gene is subject to differential splicing and results in the expression of two subtypes, Robo3.1 and Robo3.2 (Fig. 5*F*). Plasmids encoding both Robo3 subtypes were expressed in HEK293 cells (Fig. 5*G*). Cell based phosphorylation experiments demonstrate that only the Robo3.1 form is phosphorylated by PKC inside cells (Fig. 5*G*, *top panel*, *lane 1*).

Unfortunately, quantitative analysis by mass spectrometry was unsuccessful in obtaining more precise information about the identity of these putative phosphorylation sites. Therefore, we utilized peptide spot arrays as an alternate means to approach this problem (Fig. 5, *H-L*). There are twenty serine or threonine residues in the unique cytoplasmic region of Robo3.1 (Fig. 5*H*). Given the number of possible phosphosite combinations, we focused on three

segments of Robo3.1 sequence that contain consensus PKC substrate motifs (peptides A, B and C are denoted in Fig. 5, *H* and *I*). A total of sixteen immobilized peptides were evaluated (Fig. 5, *I-K*). These included wildtype sequences and peptides where alanine was substituted for putative target serines (Fig. 5*I*). UV analysis confirmed equivalent spotting efficiency for all peptides (Fig 5*L*).

In vitro phosphorylation of wild type peptides with purified PKC revealed that only peptide A was labeled (Fig 5*I*). This peptide contains Ser1330, which conforms to a consensus PKC substrate site (Fig 5*M*). Importantly, an alanine-substituted peptide analog of this sequence was not phosphorylated by this kinase (Fig. 5, *I-K*). Cell-based validation of this result was provided by analysis of a Robo3.1 S1330A mutant. As expected, wildtype Robo3.1 was efficiently phosphorylated upon stimulation of PKC (Fig. 5*N*, *top panel*, *lane 2*). In contrast, the Robo3.1 S1330A mutant was not phosphorylated by phorbol ester-mediated stimulation of endogenous PKC (Fig. 5*N*, *top panel*, *lane 4*). Loading controls confirmed equal expression of both Robo3.1 forms and immunoblot analysis using phospho-substrate antibodies detected phorbol ester stimulation of PKCs (Fig. 5*N*, *middle* and *bottom panels*). Taken together the data in figure 5 identifies Ser1330 on Robo3.1 as a target for PKC in vitro and inside cells.

Figure 5

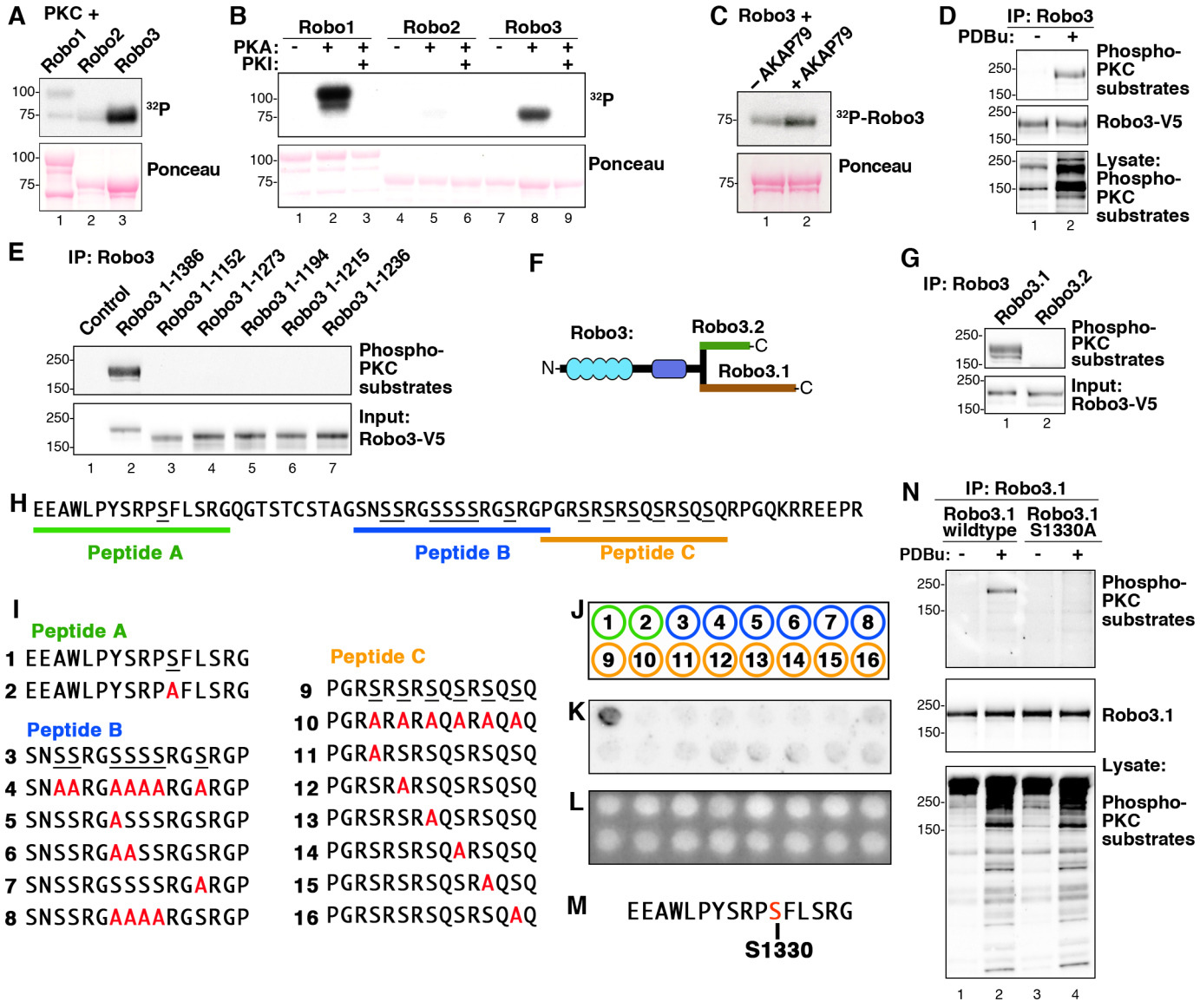
A
PKC +
Robo1
Robo2
Robo3
100-
75-
32P
Ponceau
1 2 3
B
Robo1
Robo2
Robo3
PKA:
PKI:
32P
Ponceau
1 2 3 4 5 6 7 8 9
C
Robo3 +
– AKAP79
+ AKAP79
75-
32P-Robo3
Ponceau
1 2
D
IP: Robo3
PDBu:
250-
150-
Phospho-PKC substrates
Robo3-V5
Lysate: Phospho-PKC substrates
1 2
E
IP: Robo3
Control
Robo3 1-1386
Robo3 1-1152
Robo3 1-1273
Robo3 1-1194
Robo3 1-1215
Robo3 1-1236
Phospho-PKC substrates
Input: Robo3-V5
1 2 3 4 5 6 7
F
Robo3:
Robo3.2
Robo3.1
N
C
G
IP: Robo3
Robo3.1
Robo3.2
Phospho-PKC substrates
Input: Robo3-V5
1 2
H
EEAWLPYSRPSFLSRGQGTSTCSTAGSNSSRGSSSSRGSRGPGRSRSRSQSRSQSQRPGQKRREEPR
Peptide A
Peptide B
Peptide C
I
Peptide A
1 EEAWLPYSRPSFLSRG
2 EEAWLPYSRPAFLSRG
Peptide B
3 SNSSRGSSSSRGSRGP
4 SNAARGAAAARGARGP
5 SNSSRGASSSRGSRGP
6 SNSSRGAASSRGSRGP
7 SNSSRGSSSSRGARGP
8 SNSSRGAAAARGSRGP
Peptide C
9 PGRSRSRSQSRSQSQ
10 PGRARARAQARAQAQ
11 PGRARSRSQSRSQSQ
12 PGRSRARSQSRSQSQ
13 PGRSRSRAQSRSQSQ
14 PGRSRSRSQARSQSQ
15 PGRSRSRSQSRAQSQ
16 PGRSRSRSQSRSQAQ
J
1 2 3 4 5 6 7 8
9 10 11 12 13 14 15 16
K
L
M
EEAWLPYSRPSFLSRG
S1330
N
IP: Robo3.1
Robo3.1 wildtype
Robo3.1 S1330A
PDBu:
250-
150-
Phospho-PKC substrates
Robo3.1
Lysate:
Phospho-PKC substrates
1 2 3 4

Figure 5. **PKC phosphorylates S1330 in the cytoplasmic tail of Robo3.1.** *A*, GST-Robo1CT, -Robo2CT, and -Robo3CT were phosphorylated by PKC in vitro. ^{32}P incorporation was assessed by autoradiography. *B*, GST-Robo1CT, -Robo2CT, and -Robo3CT were phosphorylated using PKA in vitro and ^{32}P incorporation was assessed by autoradiography. *C*, GST-Robo3CT was phosphorylated by PKC in vitro plus or minus purified AKAP79. *D*, Robo3 was overexpressed in HEK293 cells. Cells were stimulated with vehicle (DMSO) or 2 μM PDBu for 10 minutes. Robo3-V5 immunoprecipitations were probed using an antibody that recognizes phosphorylated consensus p-(Ser) PKC phosphorylation sites (top). *E*, Robo3 receptors containing progressive C-terminal truncations were expressed in HEK293 cells and stimulated with PDBu. V5 immunoprecipitations were immunoblotted with the phospho-PKC substrates antibody. *F*, diagram depicting the differing distal C-termini of Robo3.1 and Robo3.2. *G*, Robo3.1 and Robo3.2 were expressed in HEK293 cells. Cells were treated with PDBu and V5 immunoprecipitations of cell lysates were immunoblotted with the PKC-substrates antibody (*top*). *H*, Unique Robo3.1 C-terminal amino acid sequence. Three Robo3.1 peptides containing putative PKC phosphorylation sites are indicated. *I*, Peptides containing putative PKC sites from Robo3.1 and serine to alanine substituted peptides. *J*, Peptides 1-16 in *I* were synthesized using peptide spot array according to template. *K*, Peptide array membrane was in vitro phosphorylated with PKC and ^{32}P-ATP. Autoradiograph shows phosphorylated peptide. *L*, UV illumination of membrane shown in *K* validates equal spotting efficiency for all peptides *M*, Sequence surrounding S1330 phosphosite from peptide A. *N*, HEK293 cells expressing full length wildtype or S1330A Robo3.1 were treated with vehicle alone (DMSO) or PDBu. Robo3.1 immunoprecipitates were immunoblotted using the phospho-PKC substrates antibody to show phosphorylation of Robo3.1.

Cellular analysis of Robo3.1 phosphorylation was further examined by proximity ligation assay (PLA), a sensitive method that detects protein-protein interactions or local posttranslational modification of proteins *in situ* (95). The conceptual basis of this approach depends on the dual proximal binding of distinct antibody probes that are conjugated to complementary oligonucleotides. When the probes are within range of each other, ligation occurs to generate an amplifiable DNA circle. The resulting incorporation of fluorescent nucleotides following multiple rounds of amplification serves as a visible marker for protein-protein interactions or covalent modification of proteins that occur within a radius of 40 to 60 nm. Cells were transfected with Robo3.1 and stimulated with PDBu to activate PKCs. Proximity ligation allowed us to use the phospho-PKC substrates antibody to selectively monitor PKC activity in the vicinity of Robo3.1. Accordingly we were able to show that Robo3.1 was efficiently phosphorylated by PKC (Fig. 6, *A-C* and *G*) as compared to unstimulated controls (Fig. 6, *D-F* and *G*). Quantitation of this result is shown as the ratio of PLA signal to the single stain for Robo3.1 (Fig. 6*G*).

Finally, gene silencing was utilized to discern a role for the anchoring protein in the phosphorylation of Robo3.1 (Fig. 6, *H* and *I*). A well-characterized shRNA to AKAP79 was used to deplete the anchoring protein in HEK293 cells ((72): Fig 6*H*, *lower middle panel*, *lanes 3* and *4*). In order to accentuate the physiological relevance of this anchored phosphorylation event, we used the m_1 muscarinic receptor agonist oxotremorine-M (Oxo-M) as an activator of anchored PKC (61).

Cells expressing both Robo3 and the m_1 receptor and transfected with either control or AKAP79 shRNA were incubated for 72 h. Following treatment with vehicle or Oxo-M, Robo3 immune complexes were isolated. Phospho-Robo3.1 levels were evaluated by immunoblotting (Fig. 6*H*, *top panel*, *lanes 2* and *4*). Analysis of data from four independent experiments showed that depletion of AKAP79 significantly reduced PKC phosphorylation of Robo3.1 as assessed by densitometry (Fig. 6*I*, *columns 2* and *4*). Overall the data in figure 6 demonstrates that AKAP79 facilitates PKC phosphorylation of Robo3.1 in response to a physiological agonist.

Figure 6

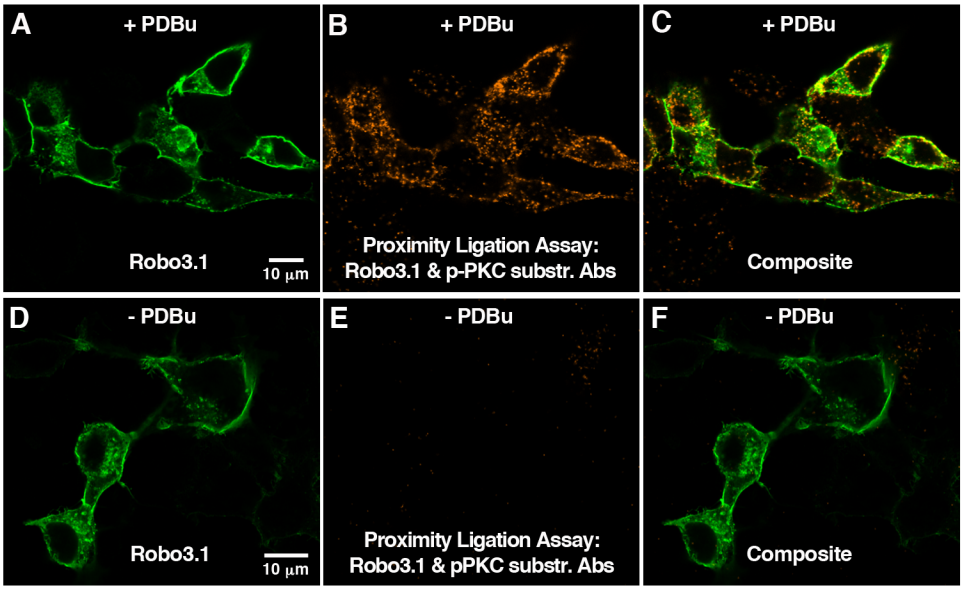
A
+ PDBu
Robo3.1
10 μm
B
+ PDBu
Proximity Ligation Assay:
Robo3.1 & p-PKC substr. Abs
C
+ PDBu
Composite
D
- PDBu
Robo3.1
10 μm
E
- PDBu
Proximity Ligation Assay:
Robo3.1 & pPKC substr. Abs
F
- PDBu
Composite

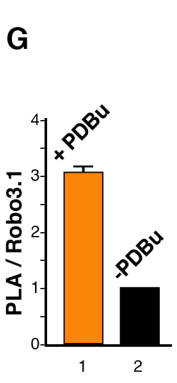
G
PLA / Robo3.1
+PDBu
-PDBu
0
1
2
3
4
1
2

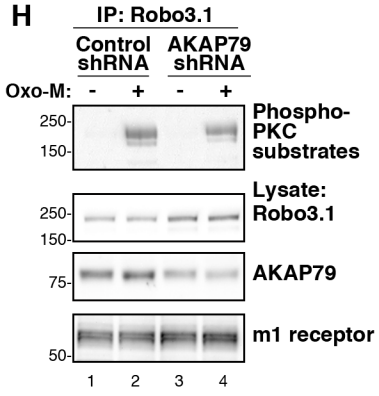
H
IP: Robo3.1
Control shRNA
AKAP79 shRNA
Oxo-M: - + - +
250-
150-
Phospho-PKC substrates
250-
150-
Lysate: Robo3.1
75-
AKAP79
50-
m1 receptor
1 2 3 4

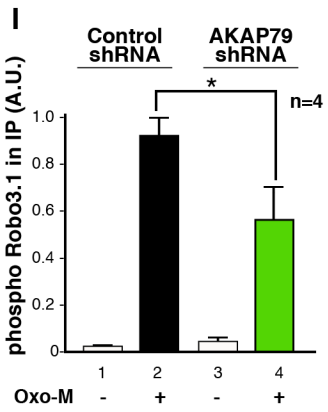
I
Control shRNA
AKAP79 shRNA
*
n=4
phospho Robo3.1 in IP (A.U.)
0
0.2
0.4
0.6
0.8
1.0
1 2 3 4
Oxo-M - + - +

Figure 6. **AKAP79 regulates the phosphorylation of Robo3.1 by PKC.** *A-F*, HEK293 cells were transfected with Robo3 and treated with PDBu (*A-C*) or vehicle (*DMSO, D-F*) for 10 minutes. Cells were incubated with a Robo3 antibody and the phospho-PKC substrates antibody and a proximity ligation assay (PLA) reaction was carried out between these two antibodies (*B, C, E, F, orange*). Cells were subsequently stained using a V5 antibody to recognize Robo3.1 (*A, C, D, F, green*). *G*, analysis of PLA signal normalized to Robo3 expression (means ± SEM, n=3, >100 cells, $p \leq 0.05$, one sample t-test). *H*, Robo3 and the m_1 muscarinic receptor were coexpressed in HEK293 cells with control or AKAP79 shRNA. Cells were treated with vehicle (H_20) or 10 μM oxotremorine-M (Oxo-M) for 2 minutes. V5 immunoprecipitations of cell lysates were immunoblotted with the PKC-substrates antibody (*top*). Robo3.1 expression (top middle), AKAP79 knockdown (bottom middle), and m_1 receptor expression (bottom) were confirmed by immunoblotting. *I*, quantification of phospho-Robo3 signal present in immunoprecipitations normalized to Robo3 expression (means ± SEM, n=4, $p \leq 0.05$, unpaired t-test).

Discussion:

The data presented in figure 5 demonstrates that Robo receptors are targets for AKAP79/150-anchored enzymes. Strikingly, Robo3 is the only member of the Roundabout family phosphorylated by PKC. The Ser1330 PKC site we identified lies within the differentially spliced C-terminus of Robo3.1. Thus, it is possible that phosphorylation at this site may contribute to Robo3.1's unique ability to silence axonal repulsion mediated by Slit-Robo signaling. Phosphorylation of Robo3.1 by AKAP79/150-anchored PKC may provide a mechanism to regulate this isoform independently from the rest of the Robo family. Further testing of S1330A mutant Robo3.1 will be needed to determine the precise importance of this site in vivo. In addition, we demonstrate that AKAP79 is required for maximal PKC phosphorylation of Robo3.1 in HEK293 cells. Once the functional significance of S1330 phosphorylation has been established, the contribution of kinase anchoring via AKAP79/150 can be investigated in vivo using existing lines of mice lacking the PKC binding site for this AKAP.

There is also some evidence that the Arg/Ser rich region present exclusively in the Robo3.1 isoform may contain additional phosphosites for other basophilic kinases. Preliminary experiments indicate that Robo3.1, but not Robo3.2 can also be phosphorylated by Akt (unpublished observations). As Robo3.1 can likewise be phosphorylated by PKA, additional work is required to assess whether these site(s) similarly lie within this region. Collectively, these results point to the C-terminus of Robo3.1 as a target for signaling pathways involving

PKC and potentially other kinases. Phosphorylation of Robo3.1 may induce conformational changes or affect interactions with binding partners. Determining these effects, as well as determining the upstream pathways that induce Robo3.1 phosphorylation, is necessary to achieve a better understanding of Robo3-mediated silencing.

Our results also show that PKA is able to phosphorylate the Robo1 receptor. As discussed in chapter 2, this kinase is required for SDF-1 inhibition of Slit-Robo signaling. While a portion of this inhibitory effect is due to PKA phosphorylation of Rho, other targets are likely involved as well. Further investigation into the effects of PKA phosphorylation on Robo1 signaling are needed to demonstrate whether this process plays a role in SDF-1 silencing. While no direct binding of AKAP79 to Robo1 was observed, our data does not rule out the presence of this anchoring protein in Robo1 complexes. For example, Robo1 and Robo2 are able to form heterodimeric complexes. Thus, multimeric protein complexes containing Robo2, AKAP79, as well as Robo1 could be assembled and may contribute to crosstalk between Robos and other pathways. This hypothesis could be tested by investigating the ability of SDF-1 to inhibit SLIT repulsion in AKAP150 -/- animals.

Chapter 4: Robo3 interacts with 14-3-3 proteins

Introduction:

The 14-3-3 family of adaptor proteins comprises a set of seven mammalian isoforms that regulate many aspects of cellular signaling (96). They are highly rigid, helical proteins that exist primarily as dimers (97). 14-3-3s interact with binding partners containing motifs incorporating phosphorylated serine or threonine residues (98). Binding of these adaptor proteins can modulate ligand function in a number of ways (99,100). Due to their dimeric nature, 14-3-3s can serve as adaptors between multiple members of a signaling complex. They can also occlude binding sites for other proteins and disrupt interactions. Similarly, 14-3-3 binding can mask targeting sequencing and result in altered target localization. In addition, 14-3-3 proteins can directly alter the activity of their binding partners. This is often achieved by inducing conformational changes in their bound ligand.

While most attention has been focused on ligand phosphorylation events leading to 14-3-3 binding, these scaffolding proteins are themselves also targeted by kinases. For instance, JNK can phosphorylate 14-3-3 proteins and disrupt their interaction with c-Abl (101). This in turn leads to an alteration in the cellular localization of c-Abl. Thus, kinase activation can also lead to disruption of 14-3-3 binding. Other kinases, including PKC, have likewise been shown to phosphorylate 14-3-3s (102).

14-3-3 proteins are widely expressed and are required for the proper regulation of many diverse processes such as cell cycle progression, apoptosis, adhesion, and cell migration (103). Recent work has also demonstrated that they play an important role in axon guidance (49). In particular, these adaptor proteins appear to modulate the balance between growth cone attraction and repulsion. PKA phosphorylation of plexin receptors generates a 14-3-3 binding site (104). The subsequent recruitment of 14-3-3 to these receptors inhibits semaphoring mediated repulsion. This is due to the displacement of the Ras2 GTPase from PlexA and subsequent inability of the receptor to inhibit Integrin-mediated adhesion.

14-3-3 expression also inhibits repulsive signaling through the Slit-Robo pathway. Inhibition of 14-3-3 interactions using the R18 competitor peptide increases the sensitivity of *Xenopus* retinal ganglion cell growth cones to Slit (105). This in turn results in decreased axonal growth. However, the mechanism for this effect is currently unclear as no interactions between Roundabout receptors and 14-3-3 proteins have been reported.

Results:

Due to our previous results indicating that AKAP79/150 can recruit PKC to the Robo3 receptor, we were curious whether PKC activation altered the makeup of this protein complex. To answer this question, we used proteomics to identify Robo3 interactors whose binding was altered following PKC activation. V5-

tagged Robo3 was expressed in HEK293 cells. After 48 hours, cells were treated with either vehicle or the PKC activator PDBu. Cell lysates were harvested and Robo3 immune complexes were purified. Following trypsin digestion and mass spectrometry analysis, a number of proteins were identified whose interaction with Robo3 was lost following PKC activation (Fig. 7). These included multiple 14-3-3 isoforms. A loss of binding was also detected to phospholipase C and the Annexin-like protein Axa2L, as well as the known Roundabout receptor binding partner Nck2.

Figure 7

IP V5:	Empty		Robo3-V5	
PDBu	-	+	-	+
Protein	**# Peptides**			
Robo3	0	0	45	44
Putative Annexin A2-like Protein	0	0	23	10
NCK Adaptor Protein 2	0	0	1	0
Phospholipase C Gamma 1	0	0	1	0
14-3-3 Theta	0	0	2	0
14-3-3 Beta	0	0	2	2
14-3-3 Beta	0	0	9	1
14-3-3 Sigma	0	0	0	1
14-3-3 Gamma	0	0	5	3
14-3-3 Epsilon	0	0	2	1
14-3-3 Eta	0	0	3	1

Figure 7. **Mass spectrometry screen identifies Robo3 interactions modulated by PKC.** HEK293 cells were transfected with empty vector or Robo3-V5. Cells were treated with either DMSO or 2 μM PDBu for 10 minutes and Robo3-V5 immune complexes were isolated. Trypsin digestions were performed and peptides were analyzed by LC-MS. Columns indicate protein name and number of peptides detected for each condition.

To confirm the putative interaction between 14-3-3 and Robo3 we overexpressed tagged versions of both proteins in HEK293 cells. Robo3 immune complexes contained 14-3-3 as assessed by western blotting (Fig. 8*A*, *top panel*, *lane 2*). In addition, Robo3 was unable to interact with the R132E 14-3-3 mutant, which is unable to form dimers (Fig. 8*A*, *top panel*, *lane 4*). This loss of interaction with monomeric 14-3-3 is consistent with many other 14-3-3 binding partners (ref). Reciprocal immunoprecipitations also confirmed the presence of Robo3 in 14-3-3 but not control immune complexes (Fig. 8*B*).

Most 14-3-3 ligands interact with an amphipathic groove present in each monomer (106). R18 peptide is an optimized disruptor that strongly binds to this binding cleft, displacing 14-3-3 binding partners. We repeated a series of Robo3 immunoprecipitations from HEK293 cell lysate in the presence and absence of this disruptor peptide. Western blotting demonstrated that R18 impaired the ability of 14-3-3 to interact with the Robo3 receptor (Fig. 8*C*).

Our previous works suggests that scaffolds such as AKAP79 often interact with only specific members of the Robo family to form distinct signaling complexes. Therefore, it was essential to investigate whether 14-3-3 was also capable of interacting with other Robo receptors. To answer this question, 14-3-3 was overexpressed along with tagged Robo1, Robo2 or Robo3 in HEK293 cells. Cell lysates were prepared and western blotting revealed that only Robo3 immune complexes contained 14-3-3 (Fig. 8*D*, *top panel*, *lane 4*). Loading controls

confirmed equal expression of all Robo family members (Fig. 8*D*, *lower middle panel*). These results suggest that 14-3-3 interacts exclusively with the Robo3 receptor.

Figure 8

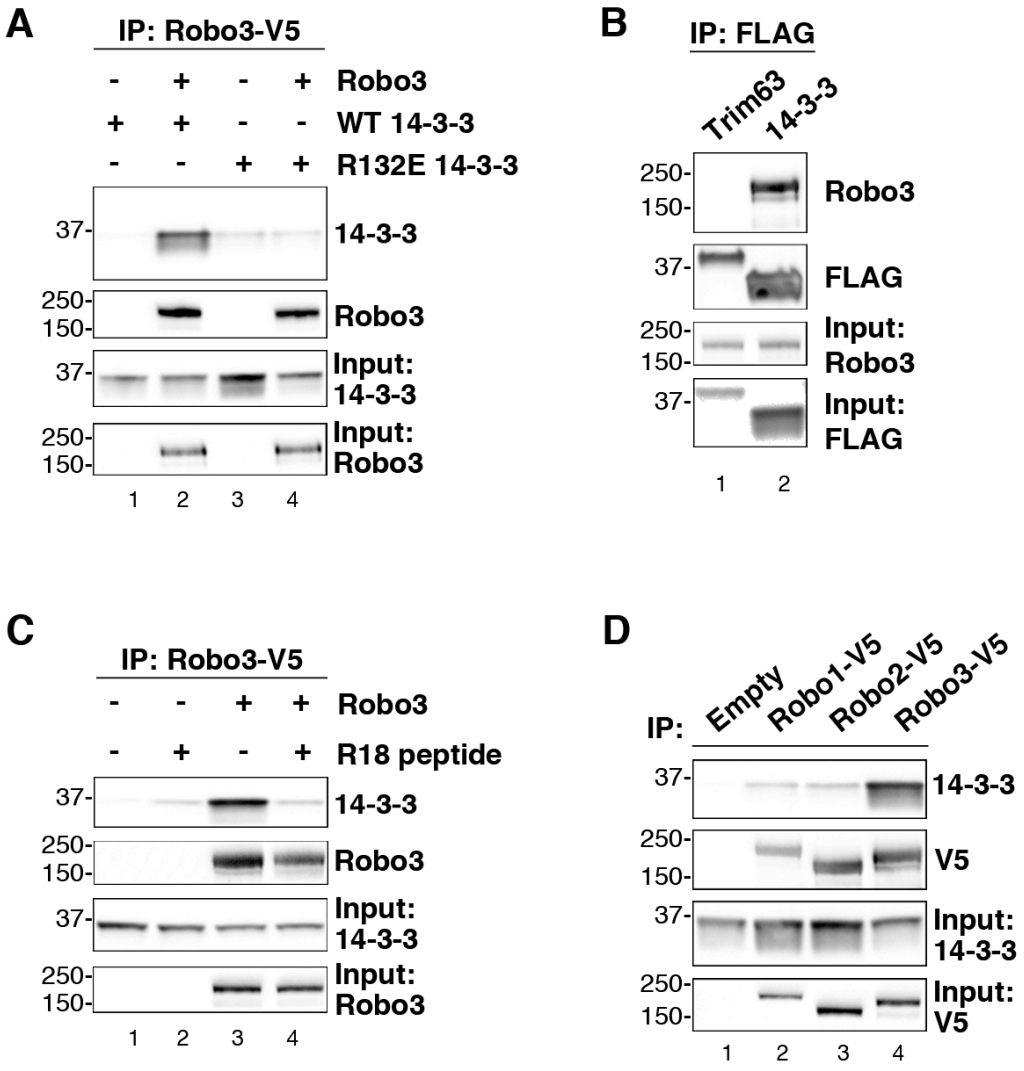

Figure 8. **Robo3 interacts with 14-3-3 proteins**. *A*, HEK293 cells were transfected with Robo3-V5 and either WT FLAG-14-3-3 or R132E FLAG-14-3-3. V5 immunoprecipitations were blotted for 14-3-3 (*top*) and Robo3 (*upper middle*). Loading controls for 14-3-3 (*lower middle*) and Robo3 (*bottom*) are included. *B*, HEK293 cells were transfected with Robo3-V5 and either FLAG-14-3-3 or control FLAG-Trim63. Reciprocal immunoprecipitations of FLAG-14-3-3 immune complexes were blotted for Robo3 *(top)* and 14-3-3 *(upper middle)*. *C*, Robo3-V5 immunoprecipitations were treated with either H_20 or R18 peptide and blotted for 14-3-3 *(top)* and Robo3 *(upper middle)*. *A*, HEK293 cells were transfected with 14-3-3 and either Robo1-V5, Robo2-V5, or Robo3-V5. V5 immunoprecipitations were blotted for 14-3-3 (*top*) and V5 (*upper middle*).

14-3-3 proteins most commonly bind to motifs containing phosphorylated serine or threonine residues in their target ligands. As Robo3 contains a number of putative 14-3-3 binding sites, we first conducted mapping experiments using versions of the receptor containing progressive truncations of the intracellular C-terminus. The shortened forms of Robo3 were expressed with 14-3-3 in HEK293 cells and binding was evaluated by western blotting analysis of Robo3 immune complexes. A Robo3 construct truncated at residue 1236 retained the ability to bind 14-3-3 (Fig. 9*A*, *top panel*, *lane 6*). However, another containing only residues 1-1215 was deficient in 14-3-3 binding (Fig. 9*A*, *top panel*, *lane 5*). This suggested that the 14-3-3 binding site on Robo3 lies between between aa 1215-1236. To confirm this hypothesis, we generated a mutant version of Robo3 lacking this region. Immune complexes of this mutant also lacked the ability to interact with 14-3-3 (Fig. 9*B*, *top panel*, *lane 3*). Scansite predicted that this region contained one high confidence 14-3-3 binding site centered around Ser1226. Site-directed mutagenesis was subsequently used to generate a Robo3 S1226A mutant, disrupting this putative binding motif. Immunoprecipitations from HEK293 cell lysate confirmed that the S1226A mutant was unable to bind 14-3-3 (Fig. 9*B*, *top panel*, *lane 4*). This data suggests that serine 1226 on Robo3 may be phosphorylated to form a 14-3-3 binding site.

Figure 9

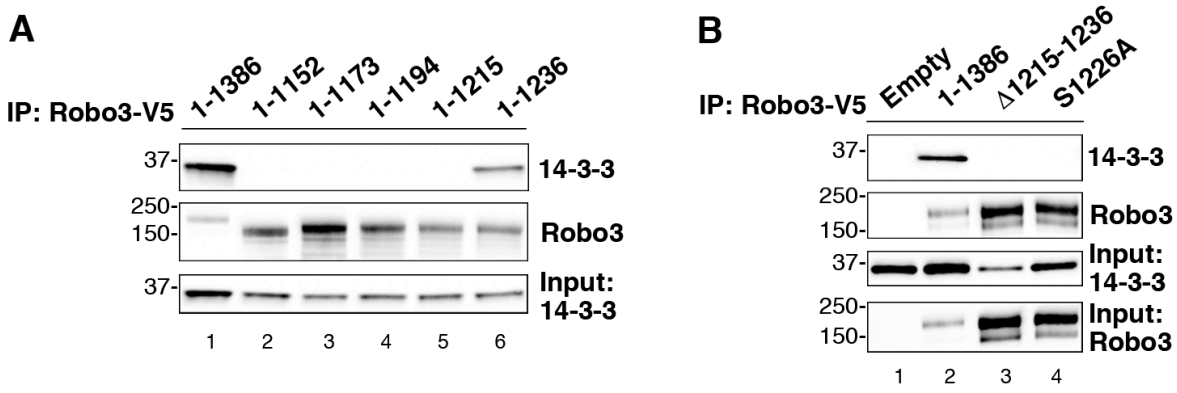

Figure 9. **Ser1226 of Robo3 is required for interaction with 14-3-3 proteins**. *A*, HEK293 cells were transfected with FLAG-14-3-3 and either full length (1-1386) or progressively truncated Robo3-V5 receptors. Numbers denote first and last amino acid present in truncated Robo3 receptors. V5 immunoprecipitations were blotted for 14-3-3 (*top*) and Robo3 (*upper middle*). *B*, FLAG-14-3-3 was expressed with either full length Robo3-V5, a version of the receptor lacking aa 1215-1236, or S1226A Robo3-V5. Immunoprecipitations of Robo3-V5 immune complexes were blotted for 14-3-3 *(top)* and Robo3-V5 *(upper middle)*.

Finally, we tested whether activation of PKC was able to disrupt the interaction of 14-3-3 with the Robo3 receptor in cells. HEK293 cells were transfected with Robo3 and 14-3-3 prior to treatment with the PKC activator PDBu. Phorbol ester stimulation significantly reduced binding of 14-3-3 to Robo3 as compared to immunoprecipitations from control cells treated with vehicle (Fig. 10, *top panel*, *lanes 2* and *3*). This effect could be blocked by treatment with the PKC inhibitor BisI (Fig. 10, *top panel*, *lane 4*). These results suggest that PKC activation may dynamically reorganize the Robo3 reorganize the Robo3 signaling complex.

Preliminary experiments suggest that this loss of 14-3-3 Robo3 binding is not due to PKC phosphorylation of S1330 on Robo3 (data not shown). Other studies have shown that 14-3-3 is also a PKC substrate and that phosphorylation of 14-3-3 can disrupt its binding to other target proteins (107). Thus, we propose that the loss of 14-3-3 binding to Robo3 upon PKC activation may be due to the phosphorylation of 14-3-3 itself. However, further experiments are need to confirm this hypothesis.

Figure 10

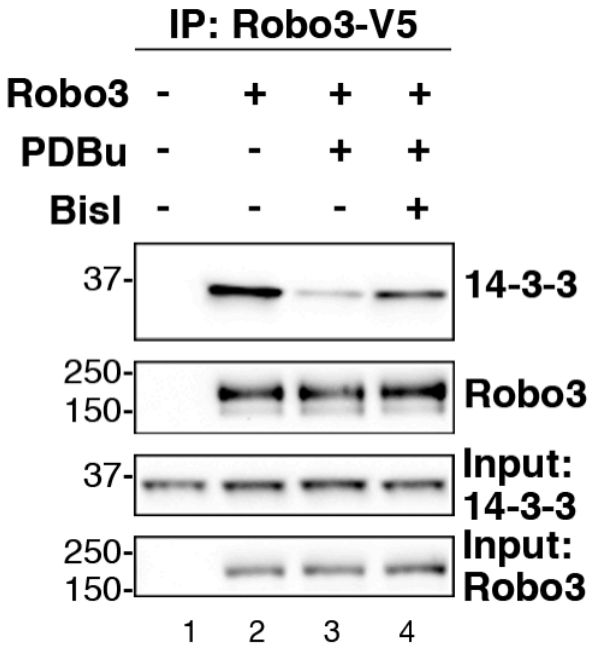

Figure 10. **PKC activation disrupts Robo3/14-3-3 binding**. *A*, HEK293 cells were transfected with FLAG-14-3-3 Robo3-V5. Cells were treated with DMSO, 2 μM PDBU for 10 minutes, or pretreated with 1 μM BIS I for 10 minutes prior to PDBu application. V5 immunoprecipitations were blotted for 14-3-3 (*top*) and Robo3 (*upper middle*).

Discussion:

Expression of 14-3-3 proteins has been shown to render growth cones less sensitive to Slit repulsion. In *Xenopus* retinal ganglion cell axons, 14-3-3 protein levels progressively decrease throughout development. The initial period of high 14-3-3 expression correlates with a stage of rapid axonal growth. Thus, it has been hypothesized that these adaptor proteins may function to dampen signaling through Roundabout receptors and promote axon elongation. Our data demonstrates that 14-3-3 proteins specifically interact with Robo3 receptor subcomplexes.

Due to Robo3's opposing function compared to Robo1 and Robo2, we are especially interested in binding partners unique to the Robo3 receptor. The ability of 14-3-3 to bind Robo3, but not other Roundabout receptors, raises the possibility that these scaffolds may contribute to Robo3's unique ability to silence conventional repulsive Slit-Robo signaling. This hypothesis is also consistent with reports showing that 14-3-3 binding to other axon guidance receptors can inhibit growth cone repulsion.

While we have demonstrated that Ser1226 is required for Robo3 binding, it remains to be shown whether S1226 must in fact be phosphorylated to create a 14-3-3 binding site. Scansite predictions suggest that possible kinase(s) responsible for phosphorylating Robo3 at this site may include Erk1 and CK1. In vitro phosphorylation of purified Robo3 using these kinases, followed by 14-3-3

pull-downs, would likely be the quickest way to demonstrate whether this interaction depends on phosphorylation of Ser1226. Elucidation of any kinases responsible for phosphorylating this site may also aid in the determination of other signaling pathways that participate in crosstalk with the Robo3 receptor. In addition, the precise mechanism leading to PKC activation and disruption of the 14-3-3 complex must still be determined. While Robo3 phosphorylation at Ser1330, a known PKC site, does not appear to play a role in this process, this kinase may instead directly phosphorylate 14-3-3 proteins to block binding.

Previous work has shown that 14-3-3 proteins regulate cytoskeletal dynamics through modulating activity of the actin-binding protein cofilin (105). 14-3-3s directly interact with cofilin, and overexpression of these scaffolds leads to increases in phosphorylated, inactive cofilin (108). As Slit-Robo signaling instead triggers phosphatase activation and dephosphorylation of cofilin, antagonism of this downstream effector may represent the mechanism of Robo3 silencing. 14-3-3 recruitment to Roundabout signaling complexes may therefore block cofilin activation, reducing the sensitivity of growth cones to Slit.

Chapter 5: Conclusion

Research on Slit-Robo signaling has elucidated many aspects of Roundabout receptor function in the decade and a half since their discovery. As Robos have no intrinsic enzymatic activity, these receptors depend on binding partners to effect changes in the actin cytoskeleton. In this thesis, I present evidence that scaffolding proteins interact with specific Robo receptor subcomplexes. This may contribute to some of the functional differences between Robo family members.

We report a novel interaction between the scaffolding protein AKAP79 and the Robo2 and Robo3 receptors. AKAP79 recruits complexes including PKA, PKC, and PP2B to these transmembrane proteins. Furthermore, immunostaining reveals that AKAP79/150 appears to co-distribute with Robo2 and Robo3, particularly at the dendritic growth cones of developing neurons. Thus, this scaffold may function to regulate dendritic development. Coexpression of AKAP79/150 with Robo2 and Robo3 is also found in the hippocampus, striatum, and olfactory tubercle of adult mice. A number of other axon guidance receptors regulate synaptic plasticity in mature neurons after their development role is complete. As AKAP79/150 plays a key role in regulating changes in synaptic strength, it will be interesting to assess whether its regulation of Slit-Robo signaling also contributes to this process.

In addition, the Robo3.1 isoform contains a PKC phosphorylation site at Ser1330 in its distal C-terminus. Data from chapter 3 demonstrates that AKAP79 facilitates the phosphorylation of Robo3.1 by PKC. Depletion of the anchoring protein suppresses phosphorylation of Robo3.1 in response to muscarinic agonists. Although little is known about Robo3 receptor subtypes there is reason to believe that Robo3.1 and Robo3.2 have divergent functions. In the developing spinal cord, Robo3.1 antagonizes repulsive axonal migration events that proceed through Robo1 and Robo2 receptors. This ability to repress canonical Slit-Robo signals is not shared by the Robo3.2 isoform. While the mechanism that accounts for the opposing functions of Robo3.1 and Robo3.2 is not clear, our data raise the possibility that PKC phosphorylation at Ser1330 of Robo3.1 may play a role in this process.

We have also determined that 14-3-3 proteins interact specifically with the Robo3 receptor. These adaptor proteins bind to Ser1226 on Robo3. Previous work in retinal ganglion cells revealed that 14-3-3s affect the sensitivity of growth cones to Slit. When 14-3-3 interactions are disrupted, axons become more responsive to Slit-Robo signaling. Our results suggest that this effect could be due to the formation of Robo3/14-3-3 complexes. Furthermore, S1226A Robo3 mutants may have an impaired ability to silence Slit-Robo signaling. Activation of PKC disrupts 14-3-3 binding to the Robo3 receptor. Therefore, this kinase may represent a mechanism through which Robo3-mediated silencing is controlled.

Taken together, these results suggests that the recruitment of scaffolding proteins to certain Robo receptor subcomplexes may confer an added element of spatiotemporal control to Slit-Robo signaling. The presence of AKAP79/150 and 14-3-3 at Robo3 receptors may also contribute to the unique signaling properties of this Robo subtype. Incorporation of these scaffolds into higher order macromolecular assemblies containing Robo receptors may expand the potential for signal integration and enzyme crosstalk between second messenger cascades and the neuronal guidance machinery.

Chapter 6: Materials and Methods

Antibodies

Antibodies used for immunoblotting included mouse anti-FLAG (Sigma-Aldrich), mouse anti-V5-HRP (Invitrogen), rabbit anti-Robo2 (Abcam), rabbit anti-AKAP150 (V088), mouse anti-RIIα (BD biosciences), mouse anti-PP2B B subunit (Abcam), mouse anti-PKCa (BD biosciences), mouse anti-His-HRP (GenScript), and rabbit anti-Phospho-Ser PKC Substrate (Cell Signaling).

Plasmid Constructs

Full length and truncated Robo1, Robo2, Robo3.1, and Robo3.2 were generated by PCR amplification and subcloned into pcDNA3.1/V5-His (Invitrogen). FLAG-AKAP79, GST-AKAP79 fragment (58,109-111), HA-muscarinic M_1 receptor, pSilencer, and AKAP79 shRNA constructs have been previously described (72). Robo1, Robo2, and Robo3.1 C-termini were cloned into pGEX6P-1 (GE) for bacterial expression. FLAG-14-3-3γ, FLAG-14-3-3γ R132E, and FLAG-Trim63 have been previously described (ref). Robo3.1 containing PreScission protease cleavage V5 tag was generated by site-directed mutagenesis.

Mass Spectrometry

Bands of interest from silver stained gels were excised and analyzed using MALDI-TOF by the OHSU proteomics shared resource.

Immunoprecipitations

HEK293 cells were transiently transfected using Mirus Transit-LT1. After 48 hours, cells were washed with cold PBS and lysed in HSE buffer (20 mM HEPES (pH 7.4), 150 mM NaCl, 5 mM EDTA, 1% Triton X-100, and protease inhibitors). For PKC phosphorylation experiments, cells were treated with DMSO or 2 μM PDBu for 10 minutes prior to harvesting and lysis buffer also contained NaF (Sigma-Aldrich) and okadaic acid (Millipore). Lysates were centrifuged at 15,000 × *g* for 20 minutes. Supernatants were incubated on nutator overnight at 4 degrees with either FLAG-agarose (Sigma-Aldrich) or anti-V5 antibody (Invitrogen) and Protein A/G-agarose (Millipore). Beads were washed 2X with HSE buffer supplemented with 10% glycerol and 500 mM NaCl and another 2X with regular HSE buffer. LDS buffer (Invitrogen) was added and samples were run on NuPage gels (Invitrogen).

HEK293 Staining

HEK293 cells were transfected with V5-Robo2 and FLAG-AKAP79 constructs. After 24 hours, coverslips were washed 3X in PBS and fixed for 20 minutes in 4% paraformaldehyde (in PBS) at room temperature. Cells were permeabilized in PBS containing 0.1% Triton X-100 and blocked for 1 hour in PBS supplemented with 10% donkey serum and 0.1% fish gelatin (Sigma). Cells were incubated with antibodies against V5 (Invitrogen; 1:1000) and FLAG (Sigma; 1:1000) overnight at 4 degrees. Coverslips were washed 3X with PBS and then incubated with Alexa Fluor-conjugated secondary antibodies for 1 hour prior to mounting.

Imaging was performed using 40× and 63× objectives on a LSM 510 META confocal microscope (Zeiss).

Immunofluorescent Staining of DIV 4 Mouse Hippocampal Neurons

For preparation of cultured hippocampal neurons, hippocampi were dissected from postnatal day 1 mice and plated at a density of 100,000 cells/well (94). After culture for 4 days in vitro (DIV), neurons were fixed in 4% paraformaldehyde for 10 minutes, washed 4X with PBS, permeabilized, and then blocked overnight in 10% donkey serum + PBS. Cells were stained with goat anti-AKAP150 (Santa Cruz; 1:200) and rabbit anti-Robo2 (Abcam; 1:500) antibodies. Cells were washed 3X with PBS and incubated for one hour at room temperature with Alexa Fluor-conjugated secondary antibodies before mounting. Neurons were imaged using an Axiovert 200M microscope (Zeiss) with a 63× objective (1.4 NA; plan-Apo) and a CoolSNAP2 (Photometrics) CCD camera. Acquisition and off-line processing were conducted using Slidebook 5.5 (Intelligent Imaging Innovations, Denver, CO). Focal plane z-stacks (spaced 0.2 μm apart) were acquired and deconvolved to discard out of focus light. Deconvolved 3D z-stacks were then collapsed to generate 2D-maximum-intensity projections.

Transfection of Hippocampal Neurons

DIV 14 mouse hippocampal neurons were transfected with V5-Robo using calcium phosphate. Cells were incubated for 24 hours prior to fixation and staining with anti-V5 (Invitrogen; 1:1000) and anti-AKAP150 (V088; 1:1000)

antibodies. Coverslips were imaged on a LSM 510 META confocal microscope (Zeiss) using 40× and 63× objectives.

GST Pull-downs

GST-Robo fusion proteins were purified from *E. coli* and left on glutathione beads. Mouse brains were homogenized in cold HSE buffer using a Polytron and cleared by centrifuging at 15,000 × *g* for 30 minutes. Brain lysate or purified protein was added and rocked overnight at 4 degrees. Beads were washed 3X with HSE buffer supplemented to contain 1M NaCl, 2X with regular HSE, and finally with PBS prior to addition of sample buffer. For PP2B pull-downs, lysates were prepared as described above and rocked with glutathione beads for 1 hour at 4 degrees. Beads were washed 3X with buffer containing 150 mM NaCl, 50 mM Tris (pH 7.5), 0.5% NP-40, and protease inhibitors before adding sample buffer. For PKC pull-downs, glutathione beads were rocked overnight with brain lysate and washed with HSE buffer as described above. 100 ng PKCβII was added to beads and incubated in 100 uL buffer containing 150 mM NaCl, 50 mM Tris (pH 7.5), 0.5% NP-40, and protease inhibitors for 1 hour. Samples were washed 3X with the same buffer prior to addition of LDS sample buffer.

RII Overlay

RII overlays were performed as described previously (79,112). In this far-western technique proteins from GST pull-downs were resolved by SDS-PAGE, transferred to nitrocellulose, and blots were subsequently overlaid with

digoxigenin-labelled RII subunit. Proteins that bound the labeled RII were identified following incubation with anti-digoxigenin antibody (Abcam).

Immunohistochemistry of Spinal Sections

E11.5 embryos were fixed in 4% paraformaldehyde for 2 hours, washed 4X with PBS, and cryoprotected in 30% sucrose in PBS overnight prior to embedding in OCT. Frozen sections were cut at 20 μm on a cryostat (Leica) and mounted onto Superfrost-plus slides (Fisher Scientific). The sections were blocked and permeabilized for 30 minutes in PBS + 0.1% Triton-X + 1% normal donkey serum (Jackson ImmunoResearch) and stained overnight at 4°C with the following primary antibodies: anti-L1Cam (Chemicon; 1:200), anti-AKAP150 (Santa Cruz; 1:500), and anti-Robo2 (Abcam; 1:500). The slides were then washed 3X in PBS and incubated with the appropriate fluorescent secondary antibody (Jackson ImmunoResearch) for 2 hours at 4°C. Finally, slides were washed 3X in PBS and mounted with Fluromount-G (Southern Biotech). Images were collected using a DMI6000B inverted microscope equipped for both widefield and spinning disc confocal fluorescent microscopy (Leica).

Immunohistochemistry of Sagittal Brain Sections

Brains from 16-week-old wildtype and AKAP150 -/- mice were fixed in formalin for 48 hours prior to paraffin embedding and sagittal sectioning at a thickness of 4 microns by the UW Pathology Research Services lab. Deparaffinized sections underwent antigen retrieval in a pressure cooker before blocking and staining

with anti-AKAP150 (V088; 1:1000 and Santa Cruz; 1:500), anti-Robo2 (Abcam; 1:500), or anti-Robo3 (R&D Systems; 1:500) antibodies. The sections were then washed 3X in PBS prior to incubation with Alexa Fluor-conjugated secondary antibodies for 1 hour at room temperature.. Sections were imaged using a DMI6000B inverted microscope equipped for both widefield and spinning disc confocal fluorescent microscopy (Leica).

Kinase Assays

For PKA kinase assays, GST-Robo fusion proteins were phosphorylated in kinase assay buffer containing 25 mM Tris pH 7.5, 0.1 mM EGTA, 10 mM $MgCl_2$, 50 μM ATP, and 0.2 μg PKA. PKC kinase assays were performed using 0.2 μg PKC, and the above buffer was supplemented with PKC activation mix (Millipore), 1 μg/mL diacylglycerol, and 10 μg/mL phosphatidylserine. Kinase reactions were stopped by washing 3X with cold HSE buffer prior to addition of LDS sample buffer.

Peptide Array

Peptides corresponding to regions of Robo3 containing potential PKC phosphosites were synthetized using an Auto-Spot Robot ASP 222 as previously described (113). Prior to phosphorylation, membranes were briefly wetted in ethanol and then incubated overnight in preincubation buffer [20 mM HEPES (pH 7.2), 100 mM NaCl, 2mM $MgCl_2$, 1 mM EDTA, 1 mM DTT, and 0.2 mg/ml BSA]. Membranes were then blocked for 1 hour at 30 degrees in the same buffer

supplemented with 1 mg/mL BSA and 30 μM ATP. Phosphorylation was carried out by incubating membrane in kinase assay buffer [25 mM Tris pH 7.5, 0.1 mM EGTA, 10 mM MgCl2, 50 μM ATP, PKC activation mix (Millipore), 1 μg/mL diacylglycerol, 10 μg/mL phosphatidylserine, and 0.2 μg PKC] for 30 minutes at 30 degrees. Following phosphorylation, membranes were washed 4 times for 15 minutes in 1 M NaCl, 3 times for 5 minutes in H_20, 3 times for 15 minutes in 5% phosphoric acid and finally 3 times for 5 minutes in H_20. Membranes were blocked for 1 hour in 5% non-fat milk and 1% BSA and incubated overnight with anti-Phospho-Ser PKC Substrate antibody (Cell Signaling).

Proximity Ligation Assay

HEK293 cells were transfected with V5-Robo3, and cultured for 24 hours prior to fixation and permeabilization in buffer containing 20 mM PIPES (pH 6.8), 10 mM EGTA, 1 mM MgCl, 0.2% Triton X-100, and 4% paraformaldehyde. Coverslips were blocked for 1 hour in PBS containing 10% donkey serum and 0.1% fish gelatin (Sigma) and then incubated overnight with anti-Robo3 (R&D Systems; 1:500) and anti-phospho-Ser PKC substrates (Cell Signaling; 1:1000) antibodies. The Duolink in situ proximity ligation reaction (Sigma-Aldrich) was carried out according to manufacturer's instructions. To identify transfected cells, coverslips were then incubated overnight with anti-V5 antibody, washed, and incubated for 1 hour at room temperature with Alexa Fluor-conjugated secondary antibody (Invitrogen). Coverslips were mounted using Prolong antifade mounting media containing DAPI (Molecular Probes) and imaged using 63× objective lens on a

DMI6000B inverted confocal fluorescent microscope (Leica). The amount of PLA signal for each condition was quantified using Metamorph software (Molecular Devices). Individual cells expressing V5-Robo3 were outlined and the integrated intensities of both the V5-Robo3 and PLA signals were recorded. The average ratio of PLA signal to V5-Robo3 was calculated for each experiment for both control and PDBu treatments. The fold change in normalized PLA/Robo3 ratio was determined and analyzed using a one sample t-test with .05 as the level of significance.

shRNA Knockdown of AKAP79

HEK293 cells were transfected with V5-Robo3, HA-m_1, and either pSilencer or AKAP79 pSilencer constructs. Cells were incubated for 72 hours post-transfection and then treated with either vehicle (H_20) or 10 μM oxotremorine-M for 2 minutes at 37 degrees. Robo3 immunoprecipitations and western blotting were performed as described above. Levels of phospho-Robo3 were determined by densitometric analysis and normalized to total Robo3 expression. Comparisons between pSilencer and AKAP79 pSilencer expressing cells were made using an unpaired t-test with .05 as the level of significance.

References:

1. Bashaw, G. J., and Klein, R. (2010) Signaling from axon guidance receptors. *Cold Spring Harbor perspectives in biology* **2**, a001941
2. Kidd, T., Brose, K., Mitchell, K. J., Fetter, R. D., Tessier-Lavigne, M., Goodman, C. S., and Tear, G. (1998) Roundabout controls axon crossing of the CNS midline and defines a novel subfamily of evolutionarily conserved guidance receptors. *Cell* **92**, 205-215
3. Moore, S. W., Tessier-Lavigne, M., and Kennedy, T. E. (2007) Netrins and their receptors. *Adv Exp Med Biol* **621**, 17-31
4. Seeger, M., Tear, G., Ferres-Marco, D., and Goodman, C. S. (1993) Mutations affecting growth cone guidance in Drosophila: genes necessary for guidance toward or away from the midline. *Neuron* **10**, 409-426
5. Kidd, T., Bland, K. S., and Goodman, C. S. (1999) Slit is the midline repellent for the robo receptor in Drosophila. *Cell* **96**, 785-794
6. Brose, K., Bland, K. S., Wang, K. H., Arnott, D., Henzel, W., Goodman, C. S., Tessier-Lavigne, M., and Kidd, T. (1999) Slit proteins bind Robo receptors and have an evolutionarily conserved role in repulsive axon guidance. *Cell* **96**, 795-806
7. Nguyen Ba-Charvet, K. T., Brose, K., Marillat, V., Kidd, T., Goodman, C. S., Tessier-Lavigne, M., Sotelo, C., and Chedotal, A. (1999) Slit2-Mediated chemorepulsion and collapse of developing forebrain axons. *Neuron* **22**, 463-473
8. Dickson, B. J., and Gilestro, G. F. (2006) Regulation of commissural axon pathfinding by slit and its Robo receptors. *Annu Rev Cell Dev Biol* **22**, 651-675
9. Park, K. W., Morrison, C. M., Sorensen, L. K., Jones, C. A., Rao, Y., Chien, C. B., Wu, J. Y., Urness, L. D., and Li, D. Y. (2003) Robo4 is a vascular-specific receptor that inhibits endothelial migration. *Dev Biol* **261**, 251-267
10. Long, H., Sabatier, C., Ma, L., Plump, A., Yuan, W., Ornitz, D. M., Tamada, A., Murakami, F., Goodman, C. S., and Tessier-Lavigne, M. (2004) Conserved roles for Slit and Robo proteins in midline commissural axon guidance. *Neuron* **42**, 213-223
11. Jaworski, A., Long, H., and Tessier-Lavigne, M. (2010) Collaborative and specialized functions of Robo1 and Robo2 in spinal commissural axon guidance. *J Neurosci* **30**, 9445-9453
12. Rajagopalan, S., Nicolas, E., Vivancos, V., Berger, J., and Dickson, B. J. (2000) Crossing the midline: roles and regulation of Robo receptors. *Neuron* **28**, 767-777
13. Sabatier, C., Plump, A. S., Le, M., Brose, K., Tamada, A., Murakami, F., Lee, E. Y., and Tessier-Lavigne, M. (2004) The divergent Robo family protein rig-1/Robo3 is a negative regulator of slit responsiveness required for midline crossing by commissural axons. *Cell* **117**, 157-169
14. Zelina, P., Blockus, H., Zagar, Y., Peres, A., Friocourt, F., Wu, Z., Rama, N., Fouquet, C., Hohenester, E., Tessier-Lavigne, M., Schweitzer, J., Roest Crollius, H., and Chedotal, A. (2014) Signaling switch of the axon

guidance receptor Robo3 during vertebrate evolution. *Neuron* **84**, 1258-1272
15. Rajagopalan, S., Vivancos, V., Nicolas, E., and Dickson, B. J. (2000) Selecting a longitudinal pathway: Robo receptors specify the lateral position of axons in the Drosophila CNS. *Cell* **103**, 1033-1045
16. Evans, T. A., and Bashaw, G. J. (2010) Functional diversity of Robo receptor immunoglobulin domains promotes distinct axon guidance decisions. *Curr Biol* **20**, 567-572
17. Spitzweck, B., Brankatschk, M., and Dickson, B. J. (2010) Distinct protein domains and expression patterns confer divergent axon guidance functions for Drosophila Robo receptors. *Cell* **140**, 409-420
18. Bashaw, G. J., and Goodman, C. S. (1999) Chimeric axon guidance receptors: the cytoplasmic domains of slit and netrin receptors specify attraction versus repulsion. *Cell* **97**, 917-926
19. Chen, Z., Gore, B. B., Long, H., Ma, L., and Tessier-Lavigne, M. (2008) Alternative splicing of the Robo3 axon guidance receptor governs the midline switch from attraction to repulsion. *Neuron* **58**, 325-332
20. Plump, A. S., Erskine, L., Sabatier, C., Brose, K., Epstein, C. J., Goodman, C. S., Mason, C. A., and Tessier-Lavigne, M. (2002) Slit1 and Slit2 cooperate to prevent premature midline crossing of retinal axons in the mouse visual system. *Neuron* **33**, 219-232
21. Whitford, K. L., Marillat, V., Stein, E., Goodman, C. S., Tessier-Lavigne, M., Chedotal, A., and Ghosh, A. (2002) Regulation of cortical dendrite development by Slit-Robo interactions. *Neuron* **33**, 47-61
22. Gibson, D. A., Tymanskyj, S., Yuan, R. C., Leung, H. C., Lefebvre, J. L., Sanes, J. R., Chedotal, A., and Ma, L. (2014) Dendrite self-avoidance requires cell-autonomous slit/robo signaling in cerebellar purkinje cells. *Neuron* **81**, 1040-1056
23. Marillat, V., Cases, O., Nguyen-Ba-Charvet, K. T., Tessier-Lavigne, M., Sotelo, C., and Chedotal, A. (2002) Spatiotemporal expression patterns of slit and robo genes in the rat brain. *J Comp Neurol* **442**, 130-155
24. Grieshammer, U., Le, M., Plump, A. S., Wang, F., Tessier-Lavigne, M., and Martin, G. R. (2004) SLIT2-mediated ROBO2 signaling restricts kidney induction to a single site. *Dev Cell* **6**, 709-717
25. Yuasa-Kawada, J., Kinoshita-Kawada, M., Rao, Y., and Wu, J. Y. (2009) Deubiquitinating enzyme USP33/VDU1 is required for Slit signaling in inhibiting breast cancer cell migration. *Proc Natl Acad Sci U S A* **106**, 14530-14535
26. Tear, G., Harris, R., Sutaria, S., Kilomanski, K., Goodman, C. S., and Seeger, M. A. (1996) commissureless controls growth cone guidance across the CNS midline in Drosophila and encodes a novel membrane protein. *Neuron* **16**, 501-514
27. Ypsilanti, A. R., Zagar, Y., and Chedotal, A. (2010) Moving away from the midline: new developments for Slit and Robo. *Development* **137**, 1939-1952

28. Hohenester, E. (2008) Structural insight into Slit-Robo signalling. *Biochem Soc Trans* **36**, 251-256
29. Hu, H. (2001) Cell-surface heparan sulfate is involved in the repulsive guidance activities of Slit2 protein. *Nat Neurosci* **4**, 695-701
30. Dickinson, R. E., and Duncan, W. C. (2010) The SLIT-ROBO pathway: a regulator of cell function with implications for the reproductive system. *Reproduction* **139**, 697-704
31. Nguyen-Ba-Charvet, K. T., Plump, A. S., Tessier-Lavigne, M., and Chedotal, A. (2002) Slit1 and slit2 proteins control the development of the lateral olfactory tract. *J Neurosci* **22**, 5473-5480
32. Rothberg, J. M., Jacobs, J. R., Goodman, C. S., and Artavanis-Tsakonas, S. (1990) slit: an extracellular protein necessary for development of midline glia and commissural axon pathways contains both EGF and LRR domains. *Genes Dev* **4**, 2169-2187
33. Seiradake, E., von Philipsborn, A. C., Henry, M., Fritz, M., Lortat-Jacob, H., Jamin, M., Hemrika, W., Bastmeyer, M., Cusack, S., and McCarthy, A. A. (2009) Structure and functional relevance of the Slit2 homodimerization domain. *EMBO Rep* **10**, 736-741
34. Delloye-Bourgeois, C., Jacquier, A., Charoy, C., Reynaud, F., Nawabi, H., Thoinet, K., Kindbeiter, K., Yoshida, Y., Zagar, Y., Kong, Y., Jones, Y. E., Falk, J., Chedotal, A., and Castellani, V. (2015) PlexinA1 is a new Slit receptor and mediates axon guidance function of Slit C-terminal fragments. *Nat Neurosci* **18**, 36-45
35. Wong, K., Ren, X. R., Huang, Y. Z., Xie, Y., Liu, G., Saito, H., Tang, H., Wen, L., Brady-Kalnay, S. M., Mei, L., Wu, J. Y., Xiong, W. C., and Rao, Y. (2001) Signal transduction in neuronal migration: roles of GTPase activating proteins and the small GTPase Cdc42 in the Slit-Robo pathway. *Cell* **107**, 209-221.
36. Hu, H., Li, M., Labrador, J. P., McEwen, J., Lai, E. C., Goodman, C. S., and Bashaw, G. J. (2005) Cross GTPase-activating protein (CrossGAP)/Vilse links the Roundabout receptor to Rac to regulate midline repulsion. *Proc Natl Acad Sci U S A* **102**, 4613-4618
37. Yang, L., and Bashaw, G. J. (2006) Son of sevenless directly links the Robo receptor to rac activation to control axon repulsion at the midline. *Neuron* **52**, 595-607
38. Bashaw, G. J., Kidd, T., Murray, D., Pawson, T., and Goodman, C. S. (2000) Repulsive axon guidance: Abelson and Enabled play opposing roles downstream of the roundabout receptor [In Process Citation]. *Cell* **101**, 703-715
39. Wills, Z., Emerson, M., Rusch, J., Bikoff, J., Baum, B., Perrimon, N., and Van Vactor, D. (2002) A Drosophila homolog of cyclase-associated proteins collaborates with the Abl tyrosine kinase to control midline axon pathfinding. *Neuron* **36**, 611-622
40. Simpson, J. H., Kidd, T., Bland, K. S., and Goodman, C. S. (2000) Short-range and long-range guidance by slit and its Robo receptors. Robo and Robo2 play distinct roles in midline guidance. *Neuron* **28**, 753-766

41. Zakrys, L., Ward, R. J., Pediani, J. D., Godin, A. G., Graham, G. J., and Milligan, G. (2014) Roundabout 1 exists predominantly as a basal dimeric complex and this is unaffected by binding of the ligand Slit2. *Biochem J* **461**, 61-73
42. Englund, C., Steneberg, P., Falileeva, L., Xylourgidis, N., and Samakovlis, C. (2002) Attractive and repulsive functions of Slit are mediated by different receptors in the Drosophila trachea. *Development* **129**, 4941-4951
43. Song, H. J., Ming, G. L., and Poo, M. M. (1997) cAMP-induced switching in turning direction of nerve growth cones. *Nature* **388**, 275-279
44. Zheng, J. Q. (2000) Turning of nerve growth cones induced by localized increases in intracellular calcium ions. *Nature* **403**, 89-93
45. Nishiyama, M., Hoshino, A., Tsai, L., Henley, J. R., Goshima, Y., Tessier-Lavigne, M., Poo, M. M., and Hong, K. (2003) Cyclic AMP/GMP-dependent modulation of Ca2+ channels sets the polarity of nerve growth-cone turning. *Nature* **423**, 990-995
46. Chalasani, S. H., Sabelko, K. A., Sunshine, M. J., Littman, D. R., and Raper, J. A. (2003) A chemokine, SDF-1, reduces the effectiveness of multiple axonal repellents and is required for normal axon pathfinding. *J Neurosci* **23**, 1360-1371
47. Guan, C. B., Xu, H. T., Jin, M., Yuan, X. B., and Poo, M. M. (2007) Long-range Ca2+ signaling from growth cone to soma mediates reversal of neuronal migration induced by slit-2. *Cell* **129**, 385-395
48. Welch, E. J., Jones, B. W., and Scott, J. D. (2010) Networking with AKAPs: context-dependent regulation of anchored enzymes. *Mol. Interv.* **10**, 86-97
49. Kent, C. B., Shimada, T., Ferraro, G. B., Ritter, B., Yam, P. T., McPherson, P. S., Charron, F., Kennedy, T. E., and Fournier, A. E. (2010) 14-3-3 proteins regulate protein kinase a activity to modulate growth cone turning responses. *J Neurosci* **30**, 14059-14067
50. Soderling, S. H., Guire, E. S., Kaech, S., White, J., Zhang, F., Schutz, K., Langeberg, L. K., Banker, G., Raber, J., and Scott, J. D. (2007) A WAVE-1 and WRP signaling complex regulates spine density, synaptic plasticity, and memory. *J Neurosci* **27**, 355-365
51. Carlson, B. R., Lloyd, K. E., Kruszewski, A., Kim, I. H., Rodriguiz, R. M., Heindel, C., Faytell, M., Dudek, S. M., Wetsel, W. C., and Soderling, S. H. (2011) WRP/srGAP3 facilitates the initiation of spine development by an inverse F-BAR domain, and its loss impairs long-term memory. *J Neurosci* **31**, 2447-2460
52. Westphal, R. S., Soderling, S. H., Alto, N. M., Langeberg, L. K., and Scott, J. D. (2000) Scar/WAVE-1, a Wiskott-Aldrich syndrome protein, assembles an actin- associated multi-kinase scaffold. *EMBO J.* **19**, 4589-4600
53. Soderling, S. H., Langeberg, L. K., Soderling, J. A., Davee, S. M., Simerly, R., Raber, J., and Scott, J. D. (2003) Loss of WAVE-1 causes

sensorimotor retardation and reduced learning and memory in mice. *Proc. Natl. Acad. Sci. U.S.A.* **100**, 1723-1728
54. Terman, J. R., and Kolodkin, A. L. (2004) Nervy links protein kinase a to plexin-mediated semaphorin repulsion. *Science* **303**, 1204-1207
55. Fenstermaker, V., Chen, Y., Ghosh, A., and Yuste, R. (2004) Regulation of dendritic length and branching by semaphorin 3A. *Journal of neurobiology* **58**, 403-412
56. Carr, D. W., Stofko-Hahn, R. E., Fraser, I. D., Bishop, S. M., Acott, T. S., Brennan, R. G., and Scott, J. D. (1991) Interaction of the regulatory subunit (RII) of cAMP-dependent protein kinase with RII-anchoring proteins occurs through an amphipathic helix binding motif. *J. Biol. Chem.* **266**, 14188-14192
57. Smith, F. D., Langeberg, L. K., and Scott, J. D. (2006) The where's and when's of kinase anchoring. *Trends Biochem Sci* **31**, 316-323
58. Klauck, T. M., Faux, M. C., Labudda, K., Langeberg, L. K., Jaken, S., and Scott, J. D. (1996) Coordination of three signaling enzymes by AKAP79, a mammalian scaffold protein. *Science* **271**, 1589-1592
59. Colledge, M., Dean, R. A., Scott, G. K., Langeberg, L. K., Huganir, R. L., and Scott, J. D. (2000) Targeting of PKA to glutamate receptors through a MAGUK-AKAP complex. *Neuron* **27**, 107-119
60. Oliveria, S. F., Dell'Acqua, M. L., and Sather, W. A. (2007) AKAP79/150 anchoring of calcineurin controls neuronal L-type Ca2+ channel activity and nuclear signaling. *Neuron* **55**, 261-275
61. Hoshi, N., Zhang, J. S., Omaki, M., Takeuchi, T., Yokoyama, S., Wanaverbecq, N., Langeberg, L. K., Yoneda, Y., Scott, J. D., Brown, D. A., and Higashida, H. (2003) AKAP150 signaling complex promotes suppression of the M-current by muscarinic agonists. *Nat. Neurosci.* **6**, 564-571
62. Fraser, I. D., Cong, M., Kim, J., Rollins, E. N., Daaka, Y., Lefkowitz, R. J., and Scott, J. D. (2000) Assembly of an A kinase-anchoring protein-beta(2)-adrenergic receptor complex facilitates receptor phosphorylation and signaling. *Curr Biol* **10**, 409-412
63. Sanderson, J. L., and Dell'Acqua, M. L. (2011) AKAP signaling complexes in regulation of excitatory synaptic plasticity. *The Neuroscientist : a review journal bringing neurobiology, neurology and psychiatry* **17**, 321-336
64. Citri, A., and Malenka, R. C. (2008) Synaptic plasticity: multiple forms, functions, and mechanisms. *Neuropsychopharmacology : official publication of the American College of Neuropsychopharmacology* **33**, 18-41
65. Lu, Y., Allen, M., Halt, A. R., Weisenhaus, M., Dallapiazza, R. F., Hall, D. D., Usachev, Y. M., McKnight, G. S., and Hell, J. W. (2007) Age-dependent requirement of AKAP150-anchored PKA and GluR2-lacking AMPA receptors in LTP. *Embo J* **26**, 4879-4890
66. Tunquist, B. J., Hoshi, N., Guire, E. S., Zhang, F., Mullendorff, K., Langeberg, L. K., Raber, J., and Scott, J. D. (2008) Loss of AKAP150

perturbs distinct neuronal processes in mice. *Proceedings of the National Academy of Sciences of the United States of America* **105**, 12557-12562
67. Weisenhaus, M., Allen, M. L., Yang, L., Lu, Y., Nichols, C. B., Su, T., Hell, J. W., and McKnight, G. S. (2010) Mutations in AKAP5 disrupt dendritic signaling complexes and lead to electrophysiological and behavioral phenotypes in mice. *PLoS One* **5**, e10325
68. Sanderson, J. L., Gorski, J. A., Gibson, E. S., Lam, P., Freund, R. K., Chick, W. S., and Dell'Acqua, M. L. (2012) AKAP150-anchored calcineurin regulates synaptic plasticity by limiting synaptic incorporation of Ca2+-permeable AMPA receptors. *J. Neurosci.* **32**, 15036-15052
69. Bhattacharyya, S., Biou, V., Xu, W., Schlüter, O., and Malenka, R. C. (2009) A critical role for PSD-95/AKAP interactions in endocytosis of synaptic AMPA receptors. *Nat. Neurosci.* **12**, 172-181
70. Dell'Acqua, M. L., Dodge, K. L., Tavalin, S. J., and Scott, J. D. (2002) Mapping the protein phosphatase-2B anchoring site on AKAP79. Binding and inhibition of phosphatase activity are mediated by residues 315-360. *J Biol Chem* **277**, 48796-48802
71. Tavalin, S. J. (2008) AKAP79 selectively enhances protein kinase C regulation of GluR1 at a Ca2+-calmodulin-dependent protein kinase II/protein kinase C site. *J Biol Chem* **283**, 11445-11452
72. Hoshi, N., Langeberg, L. K., and Scott, J. D. (2005) Distinct enzyme combinations in AKAP signalling complexes permit functional diversity. *Nat. Cell Biol.* **7**, 1066-1073
73. Efendiev, R., Samelson, B. K., Nguyen, B. T., Phatarpekar, P. V., Baameur, F., Scott, J. D., and Dessauer, C. W. (2010) AKAP79 interacts with multiple adenylyl cyclase (AC) isoforms and scaffolds AC5 and -6 to alpha-amino-3-hydroxyl-5-methyl-4-isoxazole-propionate (AMPA) receptors. *J Biol Chem* **285**, 14450-14458
74. Chan, G. C., Tonegawa, S., and Storm, D. R. (2005) Hippocampal neurons express a calcineurin-activated adenylyl cyclase. *J Neurosci* **25**, 9913-9918
75. Willoughby, D., Masada, N., Wachten, S., Pagano, M., Halls, M. L., Everett, K. L., Ciruela, A., and Cooper, D. M. (2010) AKAP79/150 interacts with AC8 and regulates Ca2+-dependent cAMP synthesis in pancreatic and neuronal systems. *J Biol Chem* **285**, 20328-20342
76. Zhang, M., Patriarchi, T., Stein, I. S., Qian, H., Matt, L., Nguyen, M., Xiang, Y. K., and Hell, J. W. (2013) Adenylyl cyclase anchoring by a kinase anchor protein AKAP5 (AKAP79/150) is important for postsynaptic beta-adrenergic signaling. *J Biol Chem* **288**, 17918-17931
77. Willoughby, D., Halls, M. L., Everett, K. L., Ciruela, A., Skroblin, P., Klussmann, E., and Cooper, D. M. (2012) A key phosphorylation site in AC8 mediates regulation of Ca(2+)-dependent cAMP dynamics by an AC8-AKAP79-PKA signalling complex. *J Cell Sci* **125**, 5850-5859
78. Dell'Acqua, M. L., Faux, M. C., Thorburn, J., Thorburn, A., and Scott, J. D. (1998) Membrane-targeting sequences on AKAP79 bind phosphatidylinositol-4, 5- bisphosphate. *EMBO J.* **17**, 2246-2260

79. Lester, L. B., Coghlan, V. M., Nauert, B., and Scott, J. D. (1996) Cloning and characterization of a novel A-kinase anchoring protein: AKAP220, association with testicular peroxisomes. *J. Biol. Chem.* **272**, 9460-9465
80. Hoshi, N., Langeberg, L. K., Gould, C. M., Newton, A. C., and Scott, J. D. (2010) Interaction with AKAP79 modifies the cellular pharmacology of PKC. *Mol. Cell* **37**, 541-550
81. Snyder, E. M., Colledge, M., Crozier, R. A., Chen, W. S., Scott, J. D., and Bear, M. F. (2005) Role for A kinase-anchoring proteins (AKAPS) in glutamate receptor trafficking and long term synaptic depression. *J Biol Chem* **280**, 16962-16968
82. Tavalin, S. J., Colledge, M., Hell, J. W., Langeberg, L. K., Huganir, R. L., and Scott, J. D. (2002) Regulation of GluR1 by the A-kinase anchoring protein 79 (AKAP79) signaling complex shares properties with long-term depression. *J. Neurosci.* **22**, 3044-3051.
83. Robertson, H. R., Gibson, E. S., Benke, T. A., and Dell'Acqua, M. L. (2009) Regulation of postsynaptic structure and function by an A-kinase anchoring protein-membrane-associated guanylate kinase scaffolding complex. *J Neurosci* **29**, 7929-7943
84. Keith, D. J., Sanderson, J. L., Gibson, E. S., Woolfrey, K. M., Robertson, H. R., Olszewski, K., Kang, R., El-Husseini, A., and Dell'acqua, M. L. (2012) Palmitoylation of A-kinase anchoring protein 79/150 regulates dendritic endosomal targeting and synaptic plasticity mechanisms. *J Neurosci* **32**, 7119-7136
85. Hoshi, N., Zhang, J. S., Omaki, M., Takeuchi, T., Yokoyama, S., Wanaverbecq, N., Langeberg, L. K., Yoneda, Y., Scott, J. D., Brown, D. A., and Higashida, H. (2003) AKAP150 signaling complex promotes suppression of the M-current by muscarinic agonists. *Nat Neurosci* **6**, 564-571
86. Cheng, E. P., Yuan, C., Navedo, M. F., Dixon, R. E., Nieves-Cintron, M., Scott, J. D., and Santana, L. F. (2011) Restoration of normal L-type Ca2+ channel function during Timothy syndrome by ablation of an anchoring protein. *Circulation research* **109**, 255-261
87. Nystoriak, M. A., Nieves-Cintron, M., Nygren, P. J., Hinke, S. A., Nichols, C. B., Chen, C. Y., Puglisi, J. L., Izu, L. T., Bers, D. M., Dell'acqua, M. L., Scott, J. D., Santana, L. F., and Navedo, M. F. (2014) AKAP150 Contributes to Enhanced Vascular Tone by Facilitating Large-Conductance Ca2+-Activated K+ Channel Remodeling in Hyperglycemia and Diabetes Mellitus. *Circ Res* **114**, 607-615
88. Kenwrick, S., Watkins, A., and De Angelis, E. (2000) Neural cell recognition molecule L1: relating biological complexity to human disease mutations. *Hum Mol Genet* **9**, 879-886
89. Chalasani, S. H., Sabol, A., Xu, H., Gyda, M. A., Rasband, K., Granato, M., Chien, C. B., and Raper, J. A. (2007) Stromal cell-derived factor-1 antagonizes slit/robo signaling in vivo. *J Neurosci* **27**, 973-980
90. Xu, H., Leinwand, S. G., Dell, A. L., Fried-Cassorla, E., and Raper, J. A. (2010) The calmodulin-stimulated adenylate cyclase ADCY8 sets the

sensitivity of zebrafish retinal axons to midline repellents and is required for normal midline crossing. *J Neurosci* **30**, 7423-7433
91. Zheng, J. Q., and Poo, M. M. (2007) Calcium signaling in neuronal motility. *Annu Rev Cell Dev Biol* **23**, 375-404
92. Horn, K. E., Glasgow, S. D., Gobert, D., Bull, S. J., Luk, T., Girgis, J., Tremblay, M. E., McEachern, D., Bouchard, J. F., Haber, M., Hamel, E., Krimpenfort, P., Murai, K. K., Berns, A., Doucet, G., Chapman, C. A., Ruthazer, E. S., and Kennedy, T. E. (2013) DCC expression by neurons regulates synaptic plasticity in the adult brain. *Cell reports* **3**, 173-185
93. Dell'Acqua, M. L., Smith, K. E., Gorski, J. A., Horne, E. A., Gibson, E. S., and Gomez, L. L. (2006) Regulation of neuronal PKA signaling through AKAP targeting dynamics. *Eur J Cell Biol* **85**, 627-633
94. Sanderson, J. L., Gorski, J. A., Gibson, E. S., Lam, P., Freund, R. K., Chick, W. S., and Dell'Acqua, M. L. (2012) AKAP150-anchored calcineurin regulates synaptic plasticity by limiting synaptic incorporation of Ca2+-permeable AMPA receptors. *J Neurosci* **32**, 15036-15052
95. Ke, R., Nong, R. Y., Fredriksson, S., Landegren, U., and Nilsson, M. (2013) Improving precision of proximity ligation assay by amplified single molecule detection. *PLoS One* **8**, e69813
96. Fu, H., Subramanian, R. R., and Masters, S. C. (2000) 14-3-3 proteins: structure, function, and regulation. *Annu Rev Pharmacol Toxicol* **40**, 617-647
97. Xiao, B., Smerdon, S. J., Jones, D. H., Dodson, G. G., Soneji, Y., Aitken, A., and Gamblin, S. J. (1995) Structure of a 14-3-3 protein and implications for coordination of multiple signaling pathways. *Nature* **376**, 188-191
98. Yaffe, M. B., Rittinger, K., Volinia, S., Caron, P. R., Aitken, A., Leffers, H., Gamblin, S. J., Smerdon, S. J., and Cantley, L. C. (1997) The structural basis for 14-3-3:phosphopeptide binding specificity. *Cell* **91**, 961-971
99. Morrison, D. (1994) 14-3-3: Modulators of signaling proteins. *Science* **266**, 56-57
100. Yaffe, M. B. (2002) How do 14-3-3 proteins work?-- Gatekeeper phosphorylation and the molecular anvil hypothesis. *FEBS Lett* **513**, 53-57
101. Yoshida, K., Yamaguchi, T., Natsume, T., Kufe, D., and Miki, Y. (2005) JNK phosphorylation of 14-3-3 proteins regulates nuclear targeting of c-Abl in the apoptotic response to DNA damage. *Nat Cell Biol* **7**, 278-285
102. Van Der Hoeven, P. C., Van Der Wal, J. C., Ruurs, P., Van Dijk, M. C., and Van Blitterswijk, J. (2000) 14-3-3 isotypes facilitate coupling of protein kinase C-zeta to Raf-1: negative regulation by 14-3-3 phosphorylation. *Biochem J* **345 Pt 2**, 297-306
103. Mhawech, P. (2005) 14-3-3 proteins--an update. *Cell Res* **15**, 228-236
104. Yang, T., and Terman, J. R. (2012) 14-3-3epsilon couples protein kinase A to semaphorin signaling and silences plexin RasGAP-mediated axonal repulsion. *Neuron* **74**, 108-121

105. Yoon, B. C., Zivraj, K. H., Strochlic, L., and Holt, C. E. (2012) 14-3-3 proteins regulate retinal axon growth by modulating ADF/cofilin activity. *Developmental neurobiology* **72**, 600-614
106. Petosa, C., Masters, S. C., Bankston, L. A., Pohl, J., Wang, B., Fu, H., and Liddington, R. C. (1998) 14-3-3zeta binds a phosphorylated Raf peptide and an unphosphorylated peptide via its conserved amphipathic groove. *J Biol Chem* **273**, 16305-16310
107. Morgan, A., and Burgoyne, R. (1992) Interaction between protein kinase C and Exo1 (14-3-3 protein) and its relevance to exocytosis in permeabilized adrenal chromaffin cells. *Biochem. J.* **286**, 807-811
108. Gohla, A., and Bokoch, G. M. (2002) 14-3-3 regulates actin dynamics by stabilizing phosphorylated cofilin. *Curr Biol* **12**, 1704-1710
109. Tasken, K. A., Collas, P., Kemmner, W. A., Witczak, O., Conti, M., and Tasken, K. (2001) Phosphodiesterase 4D and protein kinase a type II constitute a signaling unit in the centrosomal area. *J. Biol. Chem.* **276**, 21999-22002.
110. Logue, J. S., Whiting, J. L., Tunquist, B., Langeberg, L. K., and Scott, J. D. (2011) Anchored Protein Kinase A Recruitment of Active Rac GTPase. *J Biol Chem* **286**, 22113-22121
111. Gold, M. G., Stengel, F., Nygren, P. J., Weisbrod, C. R., Bruce, J. E., Robinson, C. V., Barford, D., and Scott, J. D. (2011) Architecture and dynamics of an A-kinase anchoring protein 79 (AKAP79) signaling complex. *Proc Natl Acad Sci U S A* **108**, 6426-6431
112. Carr, D. W., Hausken, Z. E., Fraser, I. D., Stofko-Hahn, R. E., and Scott, J. D. (1992) Association of the type II cAMP-dependent protein kinase with a human thyroid RII-anchoring protein. Cloning and characterization of the RII-binding domain. *J. Biol. Chem.* **267**, 13376-13382
113. Carlson, C. R., Lygren, B., Berge, T., Hoshi, N., Wong, W., Tasken, K., and Scott, J. D. (2006) Delineation of Type I Protein Kinase A-selective Signaling Events Using an RI Anchoring Disruptor. *J Biol Chem* **281**, 21535-21545